VARIABILITY OF SEDIMENT TRANSPORT AT A TIDAL WETLAND RESTORATION SITE: PRIME HOOK NATIONAL WILDLIFE REFUGE, DELAWARE

by

Kyle D. Runion

A thesis submitted to the Faculty of the University of Delaware in partial fulfillment of the requirements for the degree of Master of Science in Marine Studies

Fall 2019

VARIABILITY OF SEDIMENT TRANSPORT

AT A TIDAL WETLAND RESTORATION SITE:

PRIME HOOK NATIONAL WILDLIFE

REFUGE, DELAWARE

by

Kyle D. Runion

Approved: _____
Christopher K. Sommerfield, Ph.D.
Professor in charge of thesis on behalf of the Advisory Committee

Approved: _____
Mark Moline, Ph.D.
Chair of the Department of Marine Science and Policy

Approved: _____
Estella Atekwana, Ph.D.
Dean of the College of Earth, Ocean, and the Environment

Approved: _____
Douglas J. Doren, Ph.D.
Interim Vice Provost for Graduate and Professional Education and Dean of the Graduate College

ACKNOWLEDGMENTS

Throughout the duration of my time at the University of Delaware I have received a great deal of support and assistance for which I am grateful. Funding from the Marian Okie Fellowship at the University of Delaware and Delaware Sea Grant allowed me to conduct this research to fulfill my Master's degree. I would particularly like to thank my advisor, Dr. Chris Sommerfield for guidance and mentorship. I thank my committee members, Dr. Carlos Moffat and Dr. Bill Ullman, for their incredible support. Dr. Doug Miller provided significant assistance with data analysis and visualization for which I am thankful. This project would not have been completed without John Biddle, whose field- and lab-work expertise was invaluable. Staff at Prime Hook Refuge and the Delaware Department of Natural Resources and Environmental Control were extremely helpful and happy to share their deep knowledge of Prime Hook. In particular I thank Al Rizzo, Bart Wilson, Susan Guiteras, and Mike Mensinger. I would also like to acknowledge Scott Booth, who made great contributions to the project during his time as an REU intern at UD.

TABLE OF CONTENTS

LIST OF TABLES

LIST OF FIGURES

ABSTRACT

Prime Hook National Wildlife Refuge in Delaware contains over 10,000 acres of tidal wetlands along the coast of lower Delaware Bay. The refuge formerly contained two managed freshwater wetland impoundments, but starting in 2009 a series of coastal storms breached the coastal barrier and threatened the ecological integrity of the wetland complex. A restoration project was completed in 2016 to close the breaches and reintroduce regular tidal flow for the first time in decades. Sediment transport and accumulation are critical to maintain newly created tidal flats and stabilize reestablishing salt marsh vegetation. An observational study of sediment flux was conducted to develop a conceptual model of suspended sediment transport and inform ongoing restoration efforts. Time series of continuous flow and sediment concentration data obtained at four tidal channel locations and nearby meteorological (wind, precipitation) data were analyzed to identify mechanisms of sediment flux related to tides, wind stress, wave resuspension, and freshwater discharge. Analysis revealed that the post-restoration refuge behaves as a tidally choked coastal lagoon impacted by local and remote winds. Average suspended sediment concentrations (SSC) were high (80-130 mg/L) compared to typical tidal wetlands in the region (10-40m mg/L), perhaps due to resuspension of material from unvegetated tidal flats. High wind speeds generate high SSCs, and both wind speed and tidal action influence the discharge of water. Freshwater discharge from local creeks drove a net export of water, causing a net export in the sediment flux in fair weather conditions. Storm events created both import and export events, but export events were more prevalent. Storms accounted for 20% of the net sediment flux but 44% of the gross sediment flux, indicating that they are not the dominant mechanism but have a high potential for

sediment transport considering climate change projections predict an increase in storm intensity and frequency. Northerly or easterly winds and storm surge contributed to the import of water and sediment while southerly or westerly winds and fair weather conditions contributed to the export. Overall, the measured sediment flux for the refuge was an export of 5,296 ± 112 metric tons per year.

Chapter 1

INTRODUCTION

1.1 Sediment Transport in Tidal Wetlands

Tidal wetlands are valuable yet vulnerable ecosystems. They provide a wide array of ecosystem services, including habitat, erosion control, flood protection, water purification, and carbon sequestration (Zedler and Kercher 2005, Clarkson et al. 2013), and were valued at $193,843 per hectare per year (in 2007 USD) in a recent review paper on ecosystem services (Costanza et al. 2014). Tidal wetlands contribute 40% of the world's ecosystem services even though they only account for 1.5% of the area of the Earth (Whiting and Chanton 2001, Zedler and Kercher 2005). As transitional environments between land and sea, they face pressures from sea level rise, erosion, and subsidence (Nicholls 2004, Kirwan and Megonigal 2013).

Wetlands have historically been in decline in the United States since settlement by Europeans through land use change, including agricultural and urban development and conversion to deep water (Dahl et al. 1991). About half of total wetland area has been lost worldwide (Clarkson et al. 2013), consistent with losses between the 1780s and 1980s in the contiguous 48 states of the U.S. (Johnston 1994), and in Delaware (Dahl 1990). Future wetland area loss due to sea level rise is estimated at up to 20% by the 2080s, causing from 2 to 50 million additional people to be affected by flooding annually (Nicholls 2004).

Water, sediment, and nutrients flow in and out of tidal wetland systems from constant tidal oscillations and weather events (Fagherazzi et al. 2012). Sediment

transport characteristics can help managers understand viability and resilience of wetlands facing these pressures. Accretion of both organic and mineral material can help prevent submergence of tidal wetlands, particularly with sufficient input of externally derived fine-grained sediment (Kirwan et al. 2010, Fagherazzi et al. 2012, Weston 2014). The evolving morphology of tidal wetland complexes is determined by interplay between tidal flow dynamics, sediment transport, and growth of marsh plants (Friedrichs and Perry 2001). Tidal flow dynamics and sediment transport can be significantly influenced by weather (Moskalski and Torres 2012). Though on long timescales tidal wetlands often resemble a steady state, on shorter timescales tide and wave effects can cause net sediment transport seaward or landward (Friedrichs 2011). Physical forcing from tides, wind, and rainfall and available sources of sediment will influence the sediment transport. Because of the fluctuating direction of transport mechanisms including tides and winds, sediment transport can vary between import and export to a system depending on hydrology and climatic conditions.

Previous work on sediment flux in tidal wetlands indicates that sediment flux (defined as the product of suspended sediment concentration and water discharge) and the driving forces vary greatly, both in magnitude and direction among wetland sites. Sediment transport mechanisms include tide and wind-drive currents and freshwater inputs driven by precipitation events, and often a combination of these mechanisms may be a more powerful driver of sediment transport than any individual (Moskalski and Torres 2012). Additionally, vegetation can increase substrate stability and decrease water velocity, helping to trap sediment and reduce erosion (Stevenson et al. 1988). Ganju et al (2015) described a relationship between vegetative cover and sediment transport in that stable wetlands, defined as highly vegetated, tend to import

sediment. Unstable wetlands, or poorly vegetated wetlands with large areas of open water, tend to export sediment (Ganju et al. 2015).

The movement of water via tidal energy is an overarching sediment transport mechanism. Flood tides can carry suspended sediment through tidal creeks and into wetlands where slack tides via frictional forces reduce velocity and allow sedimentation. Similarly, ebb tides may remove sediment from the system. Slack water periods can be asymmetrical based on the tidal forcing and morphology of the wetland system, encouraging settling (Dronkers 1986). A flood or ebb dominance or the flood-ebb SSC asymmetry can indicate a net import or export of sediment (Aubrey 1986, Ganju et al. 2015). Tidal asymmetry occurs from frictional dampening of tides as they interact with basin bathymetry and topography, and cause the duration and maximum speed of the tidal current to vary between the flood and ebb periods (Dronkers 1986, Friedrichs 2011). Asymmetries in tidal current speed, along with the duration of slack water (when particles settle), can determine the direction of residual sediment transport and location of settling and deposition. If present, external water sources such as freshwater discharge, precipitation, and groundwater flow may cause ebb dominance in terms of the amount of water flow in tidal wetland complexes. Tidal range and accretion rate on U.S. coasts have been shown to be positively correlated (Stevenson et al. 1986) as velocity in the tidal creek increases with tidal range (Friedrichs 1995). Spring and neap tidal cycles can temporally influence SSC and sediment accumulation, with higher SSC during the spring cycle (Chen 2006). In a mesotidal backbarrier salt marsh in Norfolk, UK, tides alone provided sufficient sediment accumulation within the marsh to match sea level rise (French and Spencer 1993).

Storm surge can have a varying influence on sediment transport in tidal waterways and marshes, depending on the system and timing of flood/ebb tidal cycle (Friedrichs and Perry 2001, Moskalski and Sommerfield, 2013). The seasonal aspect of storm frequency and intensity and vegetative cover can cause the sediment transport regime to be dominated by storm events in the stormy season, returning to baseflow conditions in fair settings (Downing-Kunz and Schoellhamer 2013). Storms in wetland environments have been measured as both erosional and depositional: a large tidal range along with storm surge can provide a sufficient depth of water for large waves and wave-produced resuspension and export of bed sediments in the wetland (Pethick 1992). Conversely, rainfall events have been found to drive an annual import of sediment (Wolaver 1988). Nor'easter storms are low-pressure systems that travel north along the Atlantic Coast and typically display strong winds from the northeast, high precipitation, and coastal flooding (AMS 2000). These nor'easter storms are prevalent in the U.S. Mid-Atlantic region and were found to be the most important storms to cause marsh platform flooding and sedimentation in the St. Jones Estuary in Delaware (Moskalski and Sommerfield, 2013). The storm surge that these events provide can erode, deposit, or redistribute sediment in wetlands depending on storm characteristics and local geomorphology. The direction net of transport (export/import) during storms is influenced by the wind direction, timing of high wind speeds along with tides, and discharge effect from precipitation.

Wind speed, causing stress on the water surface and generating wind waves, can influence variations in SSC and thus sediment transport, particularly over intertidal flats as compared to the tidal channel (Ridderinkhof et al. 2000). In wave-dominated rather than tide-dominated conditions, the wind stress applied to surface

water can act as the major sediment transport mechanism (Janssen-Stelder 2000, French et al. 2008). Systems may be wave-dominated depending on their morphology and tidal regime or seasonally (Allen and Duffy 1998). Wind-produced sediment transport can range in scale from normal onshore breeze conditions to large-scale events such as hurricanes. Although wind waves have more potential to resuspend and transport sediment in shallow water (i.e. tidal flats), offshore wind and storm surge can be equally important in bringing water and sediment into a wetland complex.

Precipitation can increase the discharge of water in estuarine systems from direct input at the time of precipitation, elevated river discharge shortly after, followed by increased groundwater flow. This inflow of water can increase velocities, particularly on the ebb tide, and influence SSC. For example, Moskalski and Torres (2012) found that in Suisun Bay, California, precipitation and river discharge control SSC in the rainy season, between December and March.

Given that sediment transport mechanisms vary throughout the year, sediment budgets are often event-dependent and may experience seasonal variance in both the direction of sediment flux and the dominant sediment transport mechanism (Childers and Day 1990). In tide-dominated conditions, larger water flow and constant submersion of flats and the high marsh platform in winter have been reported to promote sedimentation, whereas erosion can occur from summertime immersion/emersion cycles (Deloffre et. al 2005), though large summer storms can have the opposite effect (Wolaver 1988). In a Georgia salt marsh, Letzch and Frey (1980) observed maximum sediment accumulation in summer, when storm incidence was low, and a minimum accumulation in autumn when storm occurrence was high. Nor'easter storms have been noted as a major component of sediment transport events

(Moskalski and Sommerfield 2013) and occur primarily in winter (Davis and Dolan 1993). Summertime biological activity can increase SSC in tidal creeks via bioturbation and biological growth (Hutchinson 1995) or decrease SSC by flocculation (Frostick and McCave 1979) and retention on plant surfaces (French and Spencer 1993). In a tributary of the San Francisco Bay, a landward flux of sediment in summer was caused by wind-wave resuspension, and conversely, the landward flux was caused by increased tidal action in the fall (Downing-Kunz and Schoellhamer 2013). In order to accurately describe sediment flux variability and net flux direction in a tidal wetland system, it is necessary to make observations over long periods and at high temporal resolution to capture storm events and other weather-related phenomena.

Wetlands may act as sediment sinks on long timescales (Phillips 1989), but some are sediment sources, depending on local conditions, and the literature provides examples of each. High salinity marshes in the mid-Atlantic U.S. have been determined to export sediment, likely due to a recent historical trend of reduction in the riverine fraction of the total sediment input. (Stevenson et al. 1988). Neighboring salt marshes in the Blackwater National Wildlife Refuge (Maryland, U.S.) experience opposite sediment flux directions: the Transquaking River and its associated marsh are importing sediment from strong tidal forcing, yet the nearby Blackwater River and saltmarsh are exporting under the influence of winds over open-water areas (Ganju et al. 2013). For a Norfolk (UK) saltmarsh, French and Spencer (1993) found that it served as a sediment sink and accreted mainly from tidal pumping (French and Spencer 1993).

Given the wide array of conditions a wetland system can experience, site-specific measurements and insight of local morphology and hydrology are crucial in

characterizing sediment flux conditions. This study aims to characterize sediment fluxes at the Prime Hook National Wildlife Refuge in Southern Delaware using water flow, sediment, and meteorological data collected between February 2018 and February 2019. New knowledge gained from this study has potential to aid management efforts at the refuge in the future; for example, if the wetland is not importing sediment at a rate likely to keep pace with sea level rise, planting efforts may be warranted to increase sedimentation. This study will also shed light on the effectiveness of the restoration effort described in the following section, which if successful may be duplicated at similar systems.

1.2 State of the Prime Hook Wetland Complex

1.2.1 Recent Conditions

Prime Hook National Wildlife Refuge (PHNWR) is a 10,144-acre wetland complex along the southeastern coast of Delaware. The refuge was established in 1963 by the Migratory Bird Conservation Act to protect existing coastal marshes from the threat of residential and industrial development, and to serve as a sanctuary for migratory birds. Over 300 species of birds find habitat at the refuge as well as various amphibians, fish, insects, mammals, reptiles, and plants (U.S. Fish and Wildlife Service 2013).

Historically, agriculture was the dominant use of land in Southern Delaware area, but residential development since the 1990s has caused a rise in the percentage of urban and suburban land (Tiner 2011). The eastern boundary of the refuge borders the Delaware Bay with various beachfront communities. Sussex County, within which the PHNWR is located, lost 11,271 acres of agricultural land between 2002 and 2012

(U.S. Department of Agriculture 2012). Sussex County projects to have 46,515 permanent residents and 23,960 additional seasonal residents by 2045, according to the 2018 Sussex County Comprehensive Plan, underscoring the importance of habitat conservation (Sussex County Planning & Zoning Commission 2019).

PHNWR is located in the Middle Atlantic Coastal Plain and falls within the Delaware Bay watershed. According to the EPA's level IV ecoregions, PHNWR is characterized as Delaware River Terraces and Uplands: tidal marshes and low gradient streams with a level landscape and surface soil consisting of saline marsh deposits and alluvial and estuarine sand and silts (DNREC 2015). Emergent wetlands make up 80% of the refuge acreage (U.S. Fish and Wildlife 2013). Annual average precipitation for the state of Delaware is 45 inches. Winter and spring nor'easter storms cause storm surges, high winds, and levels of precipitation, and coastal flooding (Leathers 2019).

Sea level rise is a concern in maintaining wetland area in the future. The Sea Level Rise Affecting Marsh Model (SLAMM) is a numerical model that simulates dominate wetland processes including inundation, erosion, overwash, and saturation to provide predictions of marsh viability when considering sea level rise (U.S. EPA 2019). A run of the SLAMM for the Prime Hook refuge in 2009 indicated that among various predicted sea level rise and sediment accretion rates, conversion to open water will increase in the next century (Scarborough 2009). A high sediment accretion rate in the refuge is the factor most important factor in maintaining the stability of the marsh system (Scarborough 2009).

The refuge is subdivided geographically into four management units, as shown in Figure 1. Unit I and IV are saltwater marshes, interacting with the tides from the Delaware Bay. Units II and III, in the center of the refuge, were formerly managed by

water control structures as freshwater impoundments, but when the water control structures were removed during the 2016 restoration Units II and III became more tidally influenced (Wilson et al. 2017). These units are influenced by freshwater discharge from the watershed via Prime Hook Creek and Slaughter Creek (Figure 1).

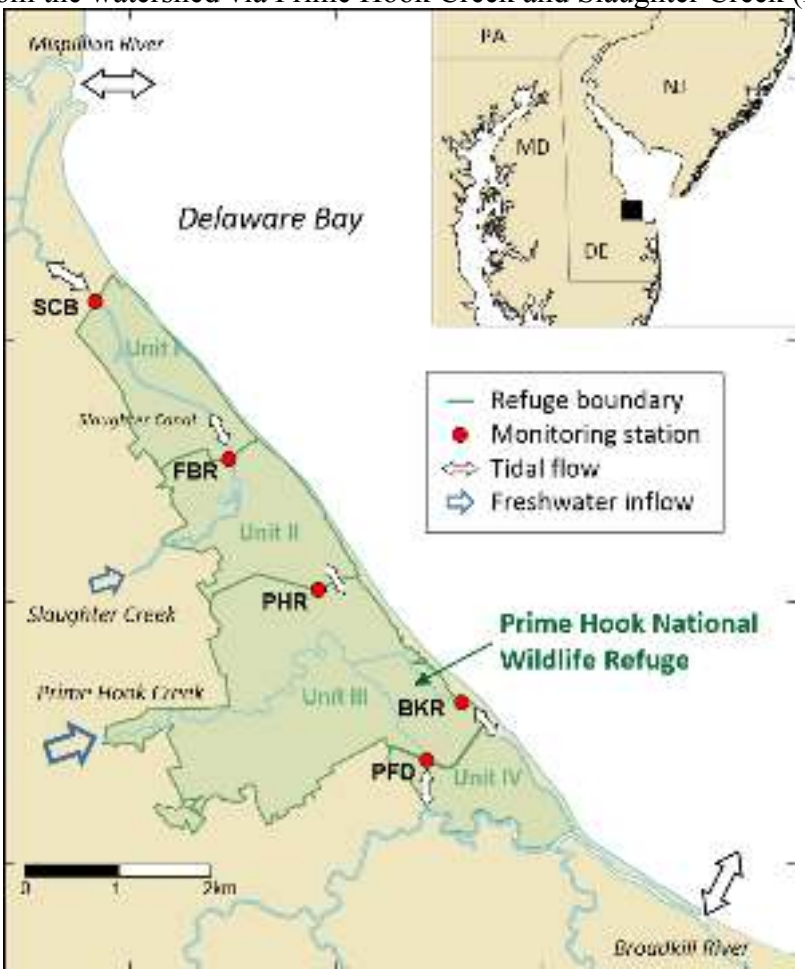

Figure 1. Map of PHNWR with unit designations, sampling station locations, and flow pathways. Station abbreviations refer to Slaughter Canal Bridge (SCB), Fowler's Beach Road (FBR), Petersfield Ditch (PFD), and Broadkill Road (BKR).

Tides from the Delaware Bay enter the refuge from the north into Unit I at the Mispillion Inlet and flow through the Cedar Creek and Slaughter Canal. Tides from the south enter the refuge into Unit IV via the Broadkill River. The tidal range is about 1.25 meters in the Delaware Bay, as measured by a NOAA tide gauge near the mouth of the Delaware Bay, but is significantly dampened as it travels into the refuge (NOAA 2019). In fair weather conditions, the tidal range near Prime Hook Road between Units II and III is about 10 cm, but water levels can change drastically from wind, precipitation, and storm surge.

With the assistance of the Coastal Programs group of the Delaware Department of Natural Resources & Environmental Control (DNREC), refuge managers established a water quality monitoring network within the four management units in October 2010. The network initially consisted of YSI data sondes, which measured salinity, water level, among other parameters at each station listed in Table 1. Equipment are further described in the following chapter (Table 2). Beginning in 2015, water flow measurements were made using Sontek Acoustic Doppler Profilers (ADP) at four of the five stations: SCB, FBR, PFD, and BKR ("USFWS Prime Hook Water Quality Metadata" 2019). Sonde and ADP equipment was managed by DNREC Coastal Programs personnel during the course of this project.

Table 1. Station code, name, coordinates (decimal degrees), and equipment utilized at each station.

Station Code	Station Name	Coordinates	Equipment
SCB	Slaughter Canal Bridge	38.49507, -75.13097	ADP, ISCO, Sonde
FBR	Fowler's Beach Road	38.87721, -75.27599	ADP, ISCO, Sonde
PHR	Prime Hook Road	38.85227, -75.25420	Sonde
PFD	Petersfield Ditch	38.81980, -75.22784	ADP, ISCO, Sonde
BKR	Broadkill Road	38.83075, -75.21937	ADP, ISCO, Sonde

Figure 2 shows boxplots of water level and salinity in the refuge ("USFWS Prime Hook Water Quality Metadata" 2019). Boxes are bounded by the 25th and 75th percentiles, with whiskers marking the 10th and 90th percentile and dots the 5th and 95th. The horizontal line represents the median. Stations are labeled on the x-axis in the boxplots corresponding to station labels in Figure 1 and Table 1. The mean water level inside the refuge is higher than that in the Delaware Bay, which drives a subtidal (mean) flow of water to the north and south from Units II and III, respectively. A gradient is apparent along the northern portion of the refuge, with the median water level falling from station PHR to stations FBR to SCB. Hence, refuge waters do not drain to the level of mean sea level at low tide. Low salinity in the center of the refuge suggests that freshwater input from Prime Hook Creek and Slaughter Creek is partly responsible for the relatively high water levels, along with the mean landward current.

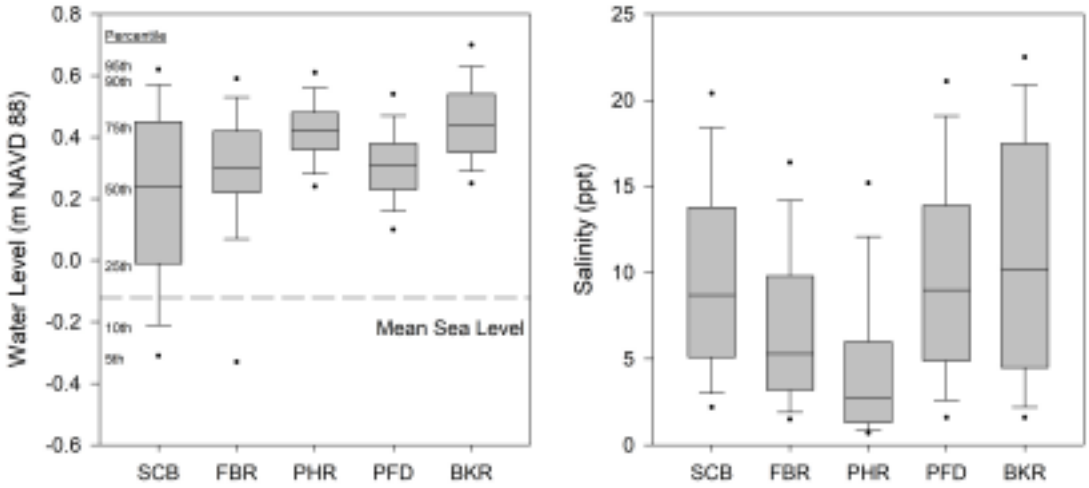

Figure 2. Boxplots of water level and salinity by station at the PHNWR. Boxes, labels, and dots are labeled with the corresponding percentile in the left plot. The mean sea level datum is from the NOAA tide gauge at Lewes. Water levels are higher and salinity is lower at the center of the refuge (PHR) than the areas closer to the Delaware Bay, suggesting that there is a non-tidal mean outflow .

1.2.2 Storm Damage

Approximately 4,000 acres of impounded wetland were created or restored between 1981 and 1988, but the coastline between these impoundments and the Delaware Bay was breached beginning in 2008 (DNREC 2015). Several coastal storms caused breaches between the Delaware Bay and the refuge in at Fowlers Beach in Unit II, most notably Hurricane Sandy in October 2012 (Wilson et al. 2017). These breaches transformed the freshwater marsh impoundments (Units II and III) into salty, shallow, open water systems and initiated rapid peat collapse (Wilson et al. 2017). This shift in the ecosystem represents a degradation in habitat for waterfowl species, and when considering increasing storm activity and rising sea levels, a freshwater

marsh in Units II and III was considered unsustainable at the time (The American Littoral Society 2012).

1.2.3 Restoration

A $38 million salt marsh restoration project under the U.S. FWS began in 2015 of which the active phase was largely completed in summer 2016 ("Marsh Restoration" 2018). The restoration involved closing the barrier breaches, restoring the about 8,900 linear feet of dunes, creating about 60 acres of marsh behind the dunes, and dredging a conveyance channel network of about 25 miles within the refuge (Wilson et al. 2017). The dredged channels are shown in Figure 3. The restored dune was raised using coarse sand to 9.8 feet, widened to over 55 feet with 100-600 feet of back-barrier platform, to capture sediment and dissipate overwash energy during storms (Wilson et al. 2017). Channels dredged ranged between 27 and 51 feet in width. Approximately 600,000 cubic yards of dredged material was applied via thin-layer application to nearby tidal flats, to restore elevation within the marsh interior and serve as on-site disposal of material (Wilson et al. 2017). In order to attain the required cross-channel area, channels were created in a box cut fashion, i.e., slightly wider and deeper than desired, knowing that they would fill somewhat with sediment from the adjacent tidal flats to a natural angle of repose (Wilson et al. 2017).

Figure 3. Map of the Prime Hook National Wildlife Refuge with refuge boundaries, station locations, and units (white) labeled. Inset map shows location relative to the Delaware Bay. Scale: 1:56,610.

Over 1000 acres of aerial seeding on exposed mudflat was conducted to promote growth of marsh plants after the dredging and spraying of sediment (Wilson et al. 2017). Approximately 255,000 *Spartina patens* and 140,000 *Spartina alterniflora* plugs were planted over 18 acres of the back-barrier platform during final stages of the restoration ("Marsh Restoration" 2018). Natural seedbanks are also expected to promote vegetation growth (Wilson et al. 2017). In general, vegetative growth on the mud flats and back-barrier platform aid in stabilizing sediment.

Through a satellite imagery analysis following the restoration, 53% and 42% of the refuge area (Units I, II, and III) were classified as open water and marsh, respectively (Susan Guiteras, personal communication, May 21, 2019). Bare ground and other vegetation comprised of the remaining acreage. Two years later in 2018, the open water area decreased to 42% and marsh increased to 52%. The site is becoming increasingly vegetated from the 2016 planting efforts and natural seed dispersal as was envisaged by the refuge managers.

1.2.4 Marsh Viability and Sea Level Rise

The sediment flux regime at Prime Hook is vital to the determination of the refuge's viability in response to the pressures of sea level rise. To avoid conversion to open water, the wetland will need to accrete material at a rate at least equal to relative sea level rise, whether that be mineral deposition from either the watershed or Delaware Bay or organic material from in-situ plant production (Kirwin and Megonigal, 2013). Due to subsidence, the rate of accretion required may be even higher (DeLaune et al., 2003). Relative sea level rise (including subsidence) at the nearest NOAA station in Lewes DE is 0.348 ± 0.023 cm/year (NOAA 2019).

Prior to the restoration, accretion rates in the refuge were found to be 0.11 to 0.54 cm/year, driven by a combination of belowground biomass growth and mineral sediment accumulation (Boyd and Sommerfield, 2016). Gathered from core samples in 2009 to 2011, these rates include measurements from Units II and III (where the accretion rates were lowest) when the water control structures were in place. Impoundments may restrict sediment accumulation (Sturdevant et al., 2002), suggesting that these rates of accretion may increase following the removal of water impoundment structures.

1.3 Research Questions

The overarching objective of this study was to quantify sediment flux in the refuge. The gross sediment flux, i.e. total amount of sediment imported and exported from the refuge during the study period, as well as the net sediment flux, i.e. total amount of sediment imported or exported to/from the refuge over the study period, will be examined. Based on factors including freshwater discharge leading to a mean export of water, low vegetative cover, and recent disturbances in the wetland (particularly channel construction), the working hypothesis of this study is that the refuge should experience a net export of sediment. To provide a framework to test this hypothesis, this study examined the following research questions:

1. Are Units II and III of the refuge exporting sediment because of low vegetative cover (e.g., Ganju et al., 2015)?
2. Does the sediment budget of the refuge differ seasonally?
3. Do storm events play a dominant role in the annual sediment accumulation?
4. Do storm events consistently transport sediment in one direction (i.e., export or import)?

Chapter 2

METHODS

2.1 Field Methods

Four data collection stations (SCB, FBR, PFD, and BKR) were located along the tidal waterways at the refuge in order to monitor water flow and sediment transport in and out of the four management units (Figures 1 and 4). A fifth station (PHR) was equipped only with a Sonde device to measure water level and salinity. Station code, name, and locations are listed in Table 1. Two stations in the northern part of the refuge, SCB and FBR, are situated along the Slaughter Canal, a tributary of the Mispillion River. SCB is located at the northern boundary of Unit I, and FBR is at the border of Units I and II. Because SCB and FBR collect information from the same waterway at the boundaries of Unit I, any difference in sediment flux between the two stations could resolve sediment gains within or losses from Unit I. The FBR station was placed to evaluate flows from Unit II. Based on examinations of water level data and field observations, little water flows between Units II and III under the Prime Hook Road bridge and drainage conduits. At the southern end of Unit III the BKR and PFD stations are both located on waterways that connect with the Broadkill River. Together, these four stations combine to allow observation of all tidal action in the refuge. Table 2 lists the source and measurement frequency of each type of data collected.

Figure 4. Sampling stations and channel outlines at Prime Hook: (a) SCB, (b) FBR, (c) PFD, and (d) BKR. Scale: 1:9,000.

Table 2. List of measurements made by the PHNWR monitoring array

Measure	Source	Frequency
SSC	ISCO	Daily
Organic Content	ISCO	Daily
Water Speed	ADP	15 minute
Discharge	ADP	15 minute
Water Level	Sonde	15 minute
Salinity	Sonde	15 minute
Wind Speed and Direction	DEOS	Daily
Precipitation	DEOS	Daily

2.1.1 Meteorological Data

Meteorological data collected by the Delaware Environmental Observing System (DEOS) is publicly available online (www.deos.udel.edu). Daily averaged onshore wind speed, direction, and precipitation data at the DEOS University of Delaware Lewes (38°47' N, -75°9' W) station was utilized in this project. In this system, wind direction is averaged through a mean of circular quantities method, wind speed is averaged arithmetically, and precipitation is summed daily. Daily averaged offshore wind speed data from the NOAA Brandywine Shoal Light, DE buoy (38°59'13 N, -75°6'47 W) is also utilized in analysis. The DEOS wind data are referred to as onshore wind and the NOAA buoy wind data are referred to as offshore wind.

2.1.2 Measuring Water Flow

Water flow (volume discharge in m^3/s) is estimated using velocity and water level measurements from a SonTek Side-Looking 1500 kHz Acoustic Doppler Profiler (ADP) at each station. The ADP, mounted near the channel bottom close to a bank, acoustically measures velocity (X-Y plane) and water level (Z plane), among other

parameters. The ADP acoustic beams are oriented perpendicular to the direction of water flow and measure both the cross-channel (X) and along-channel (Y) velocity. An acoustic vertical beam in the ADP measures the water level and is used to calculate cross-sectional area of the channel given the separately measured cross-sectional geometry of the channel. This method of discharge calculation is described by Levesque and Oberg (2012). For this study, the channel sections at the four stations were measured in 2017 and 2018. The ADPs were installed and maintained by DNREC Coastal Programs with support from the University. YSI data sondes installed at each station provided salinity and water level measurements relative to the NAVD88 vertical datum. By observing flow at these four stations, a complete view of tidal flow into and out of the refuge can be resolved. For this project, data from the sondes and ADPs were downloaded monthly by DNREC and forwarded to Dr. Sommerfield's lab group at the University of Delaware, generally on a monthly basis.

Error in ADP velocity readings, according to Simpson & Bland (2000), can be separated into random (uncorrelated) and systematic (recurring) error. The main factor in the random portion of the error is timing error, related to the difference in the time the sound wave takes to travel away from the transmitter and to the receiver (Laenen and Curtis Jr, 1998). Laenen and Curtis Jr (1998) notes that timing error decreased with increasing channel width, and estimated timing errors for a 10 m and 20 m wide channel to be 0.0754 m/s and 0.0377 m/s, respectively. Channel widths for which ADPs were located for this project were as follows: SCB 20.8 m, FBR 6.5 m, PFD 13.0 m, and BKR 13.8 m. Random error of ADP velocity for this project are near the range of 0.0754 m/s and 0.0377 m/s based on the channel width criteria of (Laenen and Curtis Jr., 1998). Systematic errors include timing error to cause an ebb or flood

bias, variation in the flow angle, variation in the path length, temperature and salinity gradients along the acoustic path, and unmeasured velocity (Simpson and Bland 2000). Systematic timing errors occur if the ADP signal threshold detector consistently measures late in one direction (Simpson and Bland 2000). Through examination of the data, no direction bias was present. Well-defined channels cause a low variation in flow angle. A steady piling installation minimizes the effect of variation in path length. Temperature and salinity gradients along the acoustic path were not observed in this project but a small channel width allows us to assume homogeneity. Unmeasured velocity behind the ADP is estimated using the one-sixth power law (SonTek 2018).

Time limitations on the project prevented ADP calibrations and error estimates. Simpson and Bland (2000) utilized similar technology and estimated an error measurement to be 0.5% of the peak tidal discharge. At the ADP stations, this corresponds to 0.24 m^3/s at SCB to 0.04 m^3/s at BKR.

During the winter months, ice flow in the creeks compromised flow data at some of the stations. In particular, some of the ADP mounts were bent, temporarily changing the orientation of the ADP. Additionally, biological fowling by barnacles (described later) compromised some of the ADP measurements. Attempts were made to regularly clean and remount the ADPs, but the ice and fouling resulted in gaps in the time series data. Note that freshwater discharge from Slaughter Creek and Prime Hook Creek was not directly measured and consequently, total freshwater inflow to the refuge by groundwater flow is unknown.

2.1.3 Suspended Sediment Concentration Samples

From 24 February 2018 to 21 February 2019, Teledyne ISCO 6712 Portable Samplers (ISCO) at the four stations collected 250 mL of water four times daily (5:00, 11:00, 16:00, and 23:00) to obtain a single composite water sample. At each station, the ISCOs were secured to a bridge above the waterway or were placed on the channel bank nearby. An intake tube extended from the ISCO pump to a mount, which was placed on the creek bottom near the center of the waterway. The intake tube was fixed to the top of the mount, located about 60 cm above the creek bottom. This location within the cross-section of the creek is representative of the average velocity (as supported by Roman (1984), whose study was conducted in Canary Creek, a tidal tributary of the Broadkill River near the University of Delaware's Lewes campus).

The ISCOs were powered by a battery, which was charged by a solar panel. During biweekly station visits, the intake mounts in the channel were inspected as needed and water samples collected. Occasional ISCO failures included power, freezing within the intake tube, and vandalism. In one instance each at the PFD and FBR station, it was suspected that the intake mount was flipped due to strong currents. These samples contained a large amount of coarse sand and were removed from analysis. Because of these issues, daily observations are not consistent throughout the study period, limiting our interpretation of the results. The number of successfully retrieved and missing samples from the period of observation are listed in Table 3.

Table 3. Period and number of observation of SSC and organic matter at each station.

Station Code	Begin Date	End Date	Total Number of Observations	Number of Observations Missing	Percent of Successful Observations
SCB	3/1/2018	2/21/2019	335	23	93%
FBR	2/24/2018	2/21/2019	296	67	77%
PFD	2/24/2018	2/21/2019	343	19	94%
BKR	2/24/2018	1/16/2019	324	3	99%

2.2 Laboratory Methods

Each daily water sample retrieved from the ISCO was filtered on a glass microfiber filter, dried at 100° C in an oven, and weighed. The volume of water filtered, ranging from 50 to 500 mL, was recorded, and with the dry sediment weight the sediment concentration was calculated in mg/L. Filters were then placed in an oven at 550° C for four and a half hours to combust organic matter (OM). The filters were cooled to room temperature and weighed again to determine the percentage of OM by loss on ignition. All bottles were cleaned as needed and rinsed with DI water before returning to the field. Two carousels of bottles for each ISCO allowed one to be in the field and one in the laboratory for analysis at all times. No replication of daily SSC and OM samples was conducted.

2.3 Data Analysis

2.3.1 Processing ADP Data

Sontek software, ViewArgonaut was used to transform the raw ADP data into velocity and discharge measurements. During the processing of raw velocity data, ADP orientation data (compass, pitch and roll) data were reviewed to ensure that there was no movement of the instrument during the data collection period. In the software,

the direction of the velocity measurements was rotated as necessary such that the maximum velocity is aligned with the channel axis. Pressure and vertical beam data were compared to check for evidence of biological fouling. The ViewArgonaut software calculates the cross-sectional area from the channel profile measurements and the water level, as measured by a vertical acoustic beam on the top of the ADP. By multiplying the velocity and channel area measurements, a rate of instantaneous discharge is calculated. The ADPs were programmed to collect velocity data at 15-minute intervals. For this study, the 15-minute velocity data were converted to 15-minute discharge, which was then averaged to yield daily discharge values.

In order to evaluate non-tidal (residual) water properties within the refuge, velocity, discharge, and water level data were low-passed filtered using a Lanczos filter with a cutoff frequency of 36 hours in MATLAB. In general, once the data have been tidally-filtered, the residual properties are related to longer term non-tidal processes, such as wind, precipitation, and storm surge.

2.3.2 Calculating Suspended Sediment Flux

Sediment flux (in dimensions of mass/time) is related to discharge, which can be calculated in multiple ways. The channel area (m^2), computed from channel width (m) and water height (m), multiplied by the instantaneous, sectionally averaged velocity (m/s) provides an instantaneous discharge (m^3/s). This discharge summed over a specified timeframe gives the total water volume passing through the tidal channel. This discharge multiplied by the suspended-sediment concentration (SSC, mg/L) is the instantaneous sediment transport rate (g/s). The instantaneous discharge and sediment transport rate can be tidally averaged to compute a time series of non-

tidal, residual discharge and transport rate. These relationships are summarized as follows:

$h * w = A$

$A * v = Q$

$Q * SSC = F$

where h = water height (m), w = width of channel (m), A = channel area (m^2), v = velocity (m/s), Q = discharge (m^3/s), SSC = suspended sediment concentration (mg/L), F = sediment flux (g/s).

To generate a time series of daily sediment flux (g/s), the 15-minute water discharge data (m^3/s) were averaged to daily values and multiplied by daily SSC (mg/L). Daily sediment fluxes were converted to a daily total and summed over the period of study to determine the cumulative sediment flux. This flux was annualized by dividing by the number of daily observations and multiplying by 365 days to arrive at a cumulative sediment flux in metric tons/year. The total flux was separated into mineral and organic fractions using loss-on-ignition measurements from the filtered water samples. These calculations are described below:

$D_d = (D_{i1} + D_{i2} + \ldots + D_{in}) / n$

$D_d * SSC = F_d$

$F_d * OC = F_{do}$

$F_d * (1 - OC) = F_{dm}$

$\sum F_{do} * 86400 \text{ seconds / day} = F_{co}$

$\sum F_{dm} * 86400 \text{ seconds / day} = F_{cm}$

$F_{co} * n_o / 365 \text{ days / year} = F_{ao}$

$F_{cm} * n_o / 365 \text{ days / year} = F_{am}$

where D_d = daily mean discharge (m^3/s), D_i = instantaneous discharge (m^3/s), n = number of instantaneous observations per day, SSC = suspended sediment concentration (mg/L), F_d = daily sediment flux (g/s), OC = organic content (%), F_{do} = daily organic sediment flux (g/s), F_{dm} = daily mineral organic sediment flux, F_{co} = study cumulative organic sediment flux (metric tons), F_{cm} = study cumulative mineral sediment flux (metric tons), n_o = number of daily observations, F_{ao} = annual organic sediment flux (metric tons), F_{am} = annual mineral sediment flux

If either discharge or SSC data were missing for a day or days, the flux could not be calculated, resulting in gaps in the time series. Uncertainty of the filtered water samples for SSC and OM was calculated by triplicate measurements of random samples. These measurements resulted in a standard error of 1.7 mg/L or 2.3% of the SSC and 1.3 percentage points or 6.4% of the OM. The standard error of the sediment fluxes was calculated by converting the SSC standard error (mg/L) to the cumulative unit (metric tons), summing by the absolute value, and annualizing (tons/year).

Chapter 3

RESULTS

A summary of the collected data is available in Table 4. This table lists the maximum, minimum, mean, and standard deviation of the velocity, water level, discharge, SSC, and OM at each station. In the table, the maximum flood and ebb measurements are listed rather than minimum for velocity and discharge. For the remainder of this thesis, measurements of velocity, discharge, and sediment flux are presented with positive values referring to ebb/seaward movements, or exports, and negative values referring to flood/landward movements, or imports. Reported mean velocity and mean discharge represent the average over both ebb and flood directions. The number days with complete observations, during which both SSC and discharge data are available, for each station are listed in Table 3. Each parameter is further described in the following sections.

Table 4. Summary of water flow and sediment data. In order to display both seaward/ebb and landward/flood characteristics for velocity and discharge, a separate header is used.

Parameter	Station	Ebb Max	Flood Max	Mean	St. Dev.
Velocity	SCB	1.13	1.01	0.08	0.49
(m/s)	FBR	0.88	0.54	0.03	0.18
	PFD	0.66	1.09	0.10	0.36
	BKR	0.50	0.36	0.05	0.19
Discharge	SCB	33.02	47.79	0.47	16.8
(m^3/s)	FBR	6.96	13.31	0.42	2.4
	PFD	11.25	7.64	0.25	3.4
	BKR	6.22	8.39	0.65	2.7
Parameter	Station	Max	Min	Mean	St. Dev.
Water Level	SCB	0.94	-0.75	0.21	0.30
(m NAVD88)	FBR	0.78	-0.79	0.28	0.24
	PFD	0.79	-0.23	0.31	0.12
	BKR	0.96	0.01	0.45	0.14
SSC	SCB	452.0	25.0	104.0	53.7
(mg/L)	FBR	403.0	22.6	106.6	60.6
	PFD	854.0	22.8	127.3	133.9
	BKR	1108.0	20.8	86.4	75.7
OM	SCB	38.3	5.30	21.0	4.5
(%)	FBR	33.9	11.2	19.0	3.5
	PFD	47.2	14.8	24.6	4.6
	BKR	45.7	14.0	23.4	4.9

3.1 Water Flow

Tidal and freshwater pathways of water flow are illustrated in Figure 1. Tidal water enters the refuge through the Mispillion and Broadkill Rivers and then enters the refuge and travels past sampling stations SCB, FBR (Mispillion), PFD, and BKR (Broadkill). Freshwater flows into the system from the Slaughter and Prime Hook Creeks into Units II and III, respectively. As shown in Figure 2, freshwater input

causes a higher water level within the refuge and a mean seaward water flow driven by gravity is presumed.

3.1.1 Velocity

Time series of instantaneous and tide-filtered (residual) velocity are shown in Figure 5. The average instantaneous velocity through the sampling period was positive at each station and ranged from 0.036 m/s at FBR to 0.084 m/s at PFD. The arithmetic average of the absolute value of velocity (to remove oscillating tidal effect) ranged from 0.15 m/s at FBR to 0.43 m/s at SCB. During the period of observations, the maximum landward velocity measured was 1.09 m/s at PFD and the maximum seaward velocity was 1.13 m/s at SCB. The largest range in terms of landward-seaward velocity among stations occurred was 2.14 m/s at SCB, while the smallest range measured 0.86 m/s at BKR.

Biological fowling occurred on ADP sensors and appeared to compromise the quality of velocity measurements at the PFD station from 9/10/2018 to 12/27/2018, and at the BKR station from 10/27/2018 to 11/16/2018. Barnacles grew on the ADPs and limited their ability to transmit and receive sound signals. These measurements were removed from analysis. Other data gaps are caused by physical shifting of the ADP, typically due to ice flow or debris.

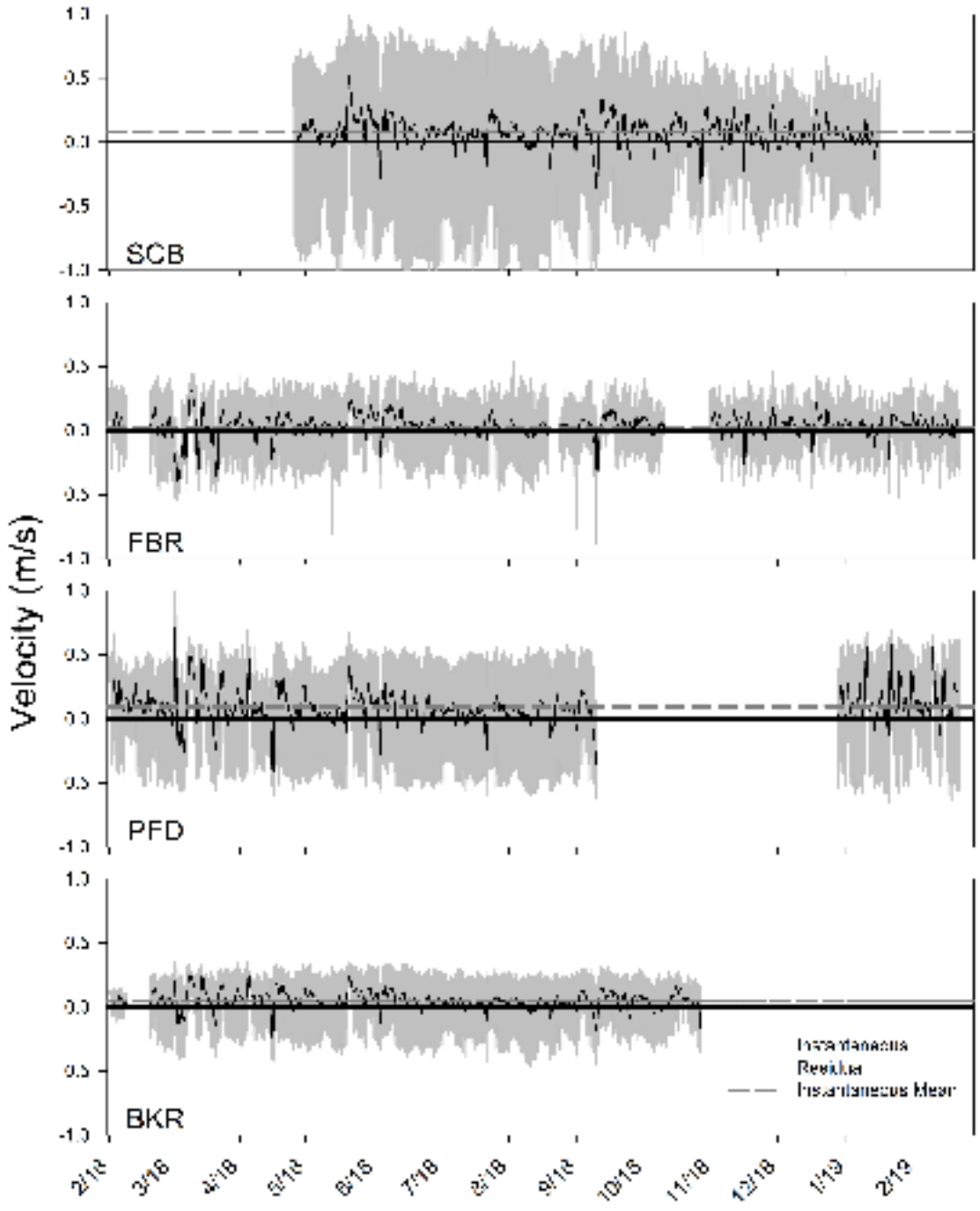

Figure 5. Instantaneous, mean instantaneous, and residual velocity at each station. Positive values represent the seaward direction and negative represent the landward direction. The mean instantaneous velocity at each station is slightly positive (seaward-directed current).

3.1.2 Water Level

A time series of water level throughout the duration of the project, referenced to the NAVD88 datum, is presented in Figure 6. Malfunctions in Sonde equipment caused some gaps in the time series at the FBR and BKR stations. The instantaneous data capture the semi-diurnal and spring-neap tidal cycle. Residual data are obtained by conducting a low-passed filter on the data to remove the tidal influence and shows subtidal water-level variations caused by storm surge, wind, or rainfall. Water-level variations were dominated by subtidal effects in Units II and III (stations FBR, PFD, and BKR), while areas of the refuge closer to the Delaware Bay (SCB) experienced a stronger semi-diurnal and spring-neap variation in water level due to the tides. The tide was slightly dampened upon entering the Mispillion River from the Delaware Bay and at the SCB station, from an average range of 1.25 m to about 0.8 m (NOAA 2019). Upon entering Unit II, the tide was significantly dampened and has a range of about 0.1 m at the FBR station. Along the Broadkill River tidal entrance, tides were similarly dampened to a range of about 0.2 m at the PFD and BKR stations (Unit III entrance).

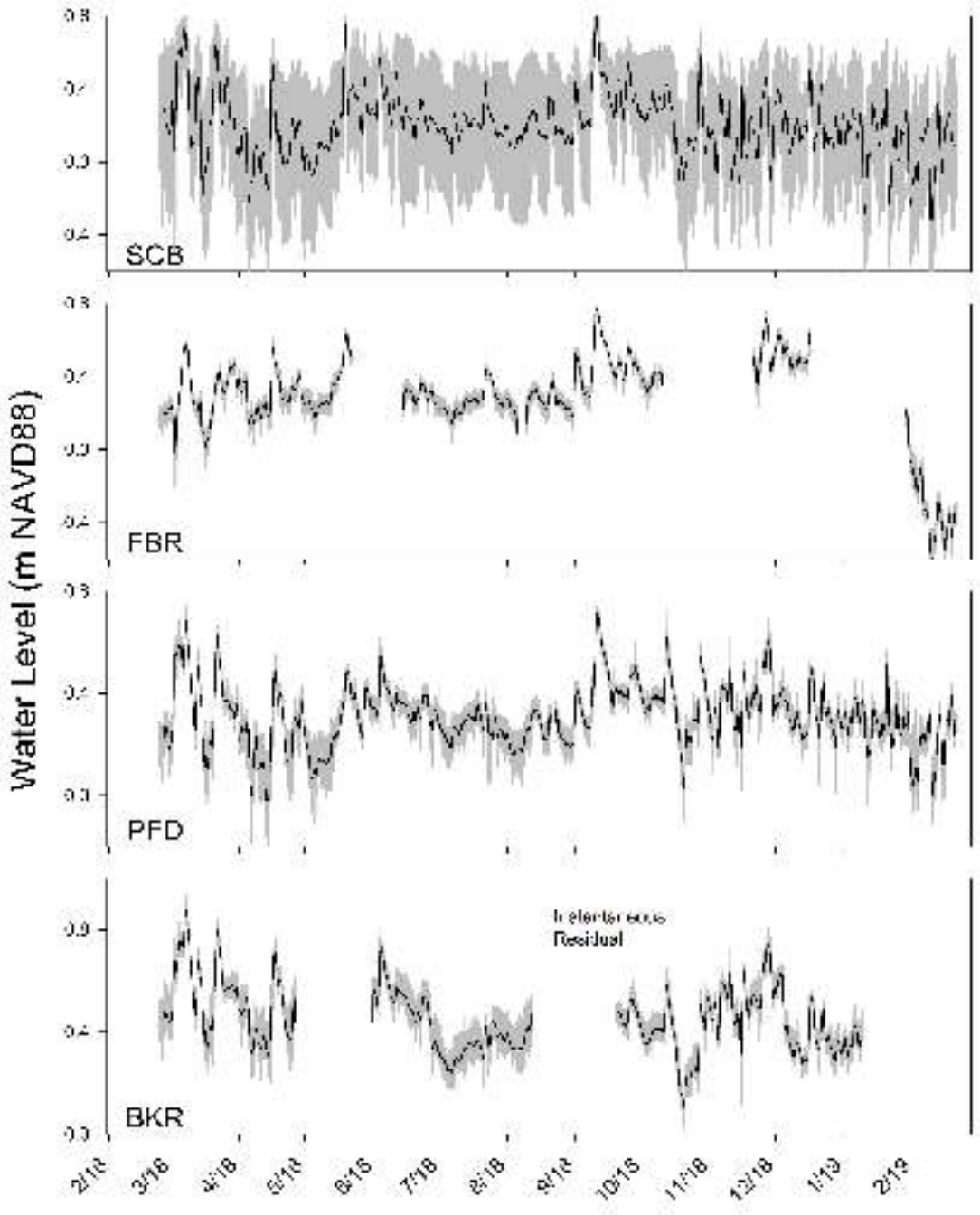

Figure 6. Instantaneous and residual water level (meters NAVD88) at each station. Note the varying scales on the y-axis.

3.1.3 Discharge

Volume discharge of water (calculated in m^3/s by multiplying velocity and cross-sectional area within SonTek Argonaut software) is shown in Figure 7. The mean instantaneous discharge at each station was positive, representing a non-tidal export current, and ranged from 0.319 m^3/s at FBR to 0.623 m^3/s at BKR. The maximum instantaneous ebb and flood discharge over the time series were each measured at SCB, at 33.0 m^3/s and - 47.8 m^3/s, respectively, representing a range of 80.8 m^3/s. The smallest range of ebb and flood discharge among stations was 14.6 m^3/s at BKR.

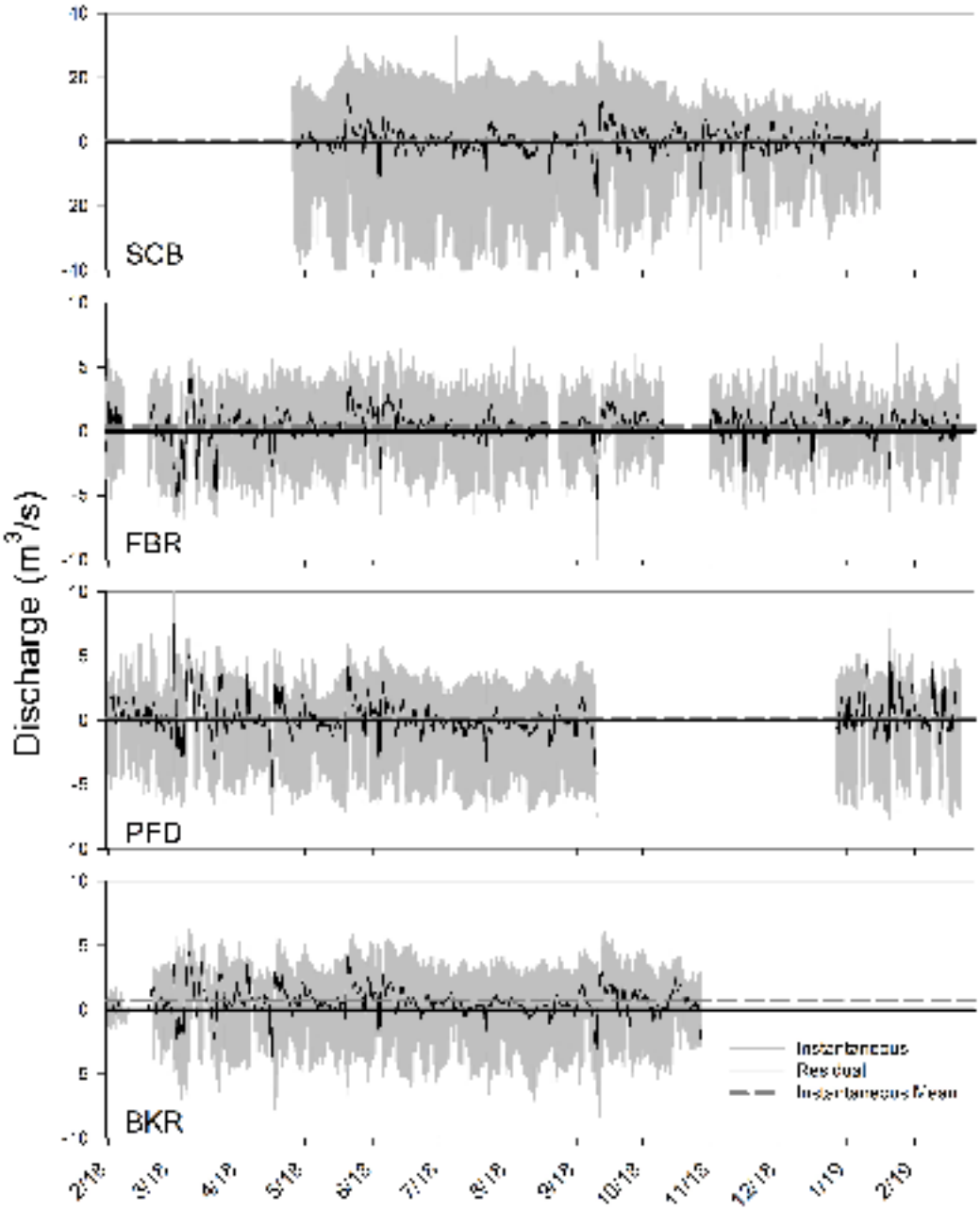

Figure 7. Instantaneous, mean instantaneous, and residual discharge at each station. Positive values represent the ebb and negative represent the flood. The mean instantaneous discharge is slightly positive (ebb) at each station.

Plotting the discharge as monthly averages (Figure 8) reveals a slight seasonal trend. In Figure 8, positive values represent an export of water whereas negative values represent an import of water into the refuge. Monthly mean discharge generally exhibited larger exports in the winter and smaller exports or small imports during the summer at the FBR, PFD, and BKR stations. This trend was not observed at the SCB station, which is closest to Delaware Bay. Apparently, in summer more water was evapotranspired within the refuge and upstream in the watershed, reducing fresh water inflow and mean discharge. Precipitation from storms in the winter caused an increase in freshwater inflow and mean discharge.

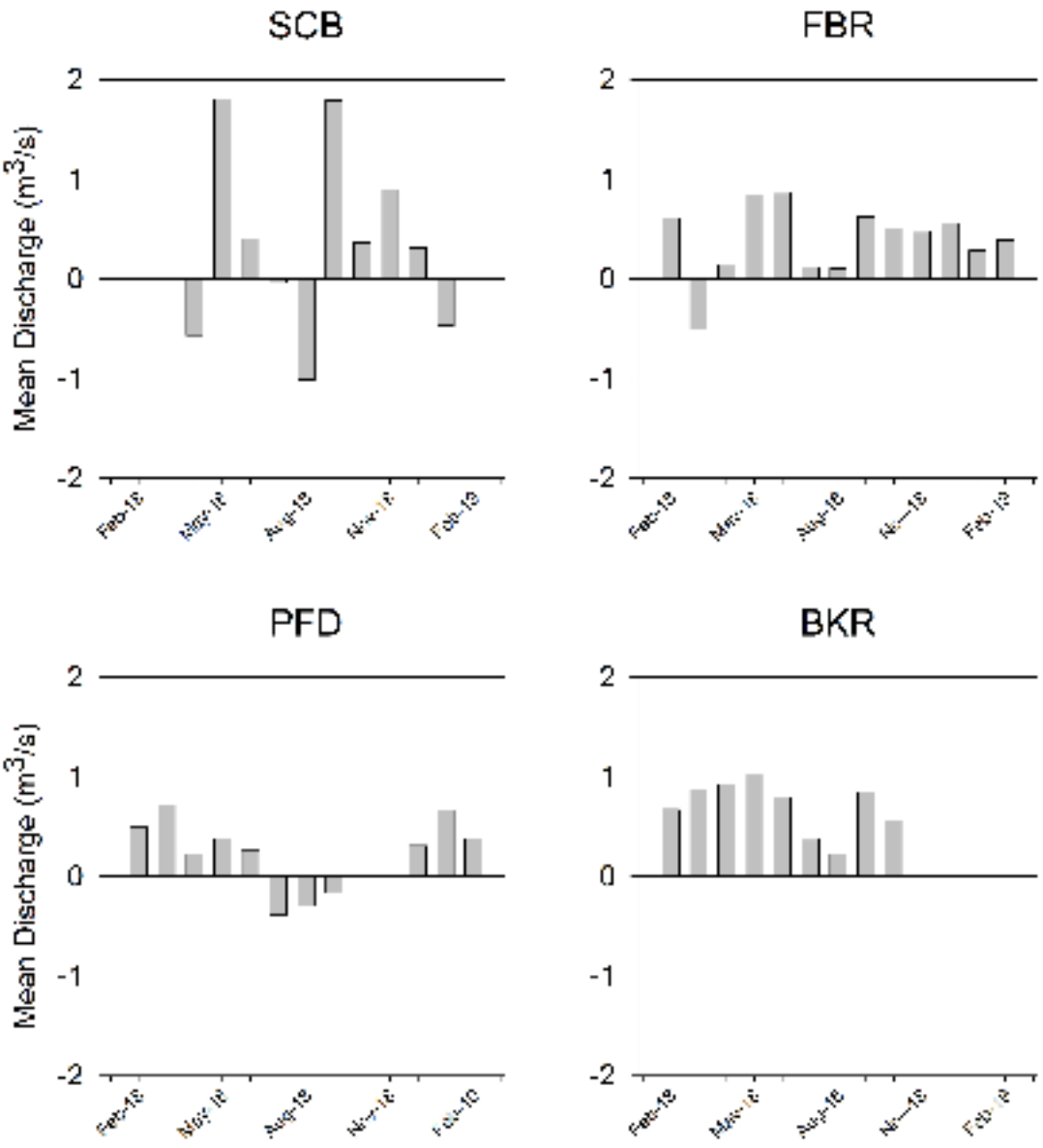

Figure 8. Mean monthly discharge at each station. A slightly seasonal trend is evident at the FBR, PFD, and BKR stations.

3.2 Suspended Sediment

3.2.1 Suspended Sediment Concentration and Organic Matter

The number of daily observations of SSC and OM are listed in Table 2. Time series of SSC and OM for all stations are shown in Figures 9 and 10, respectively. Missing values in these plots show the dates of ISCO malfunctions. Winter months (November - April) exhibit larger variability in SSC compared to the summer months (May – October) at each station.

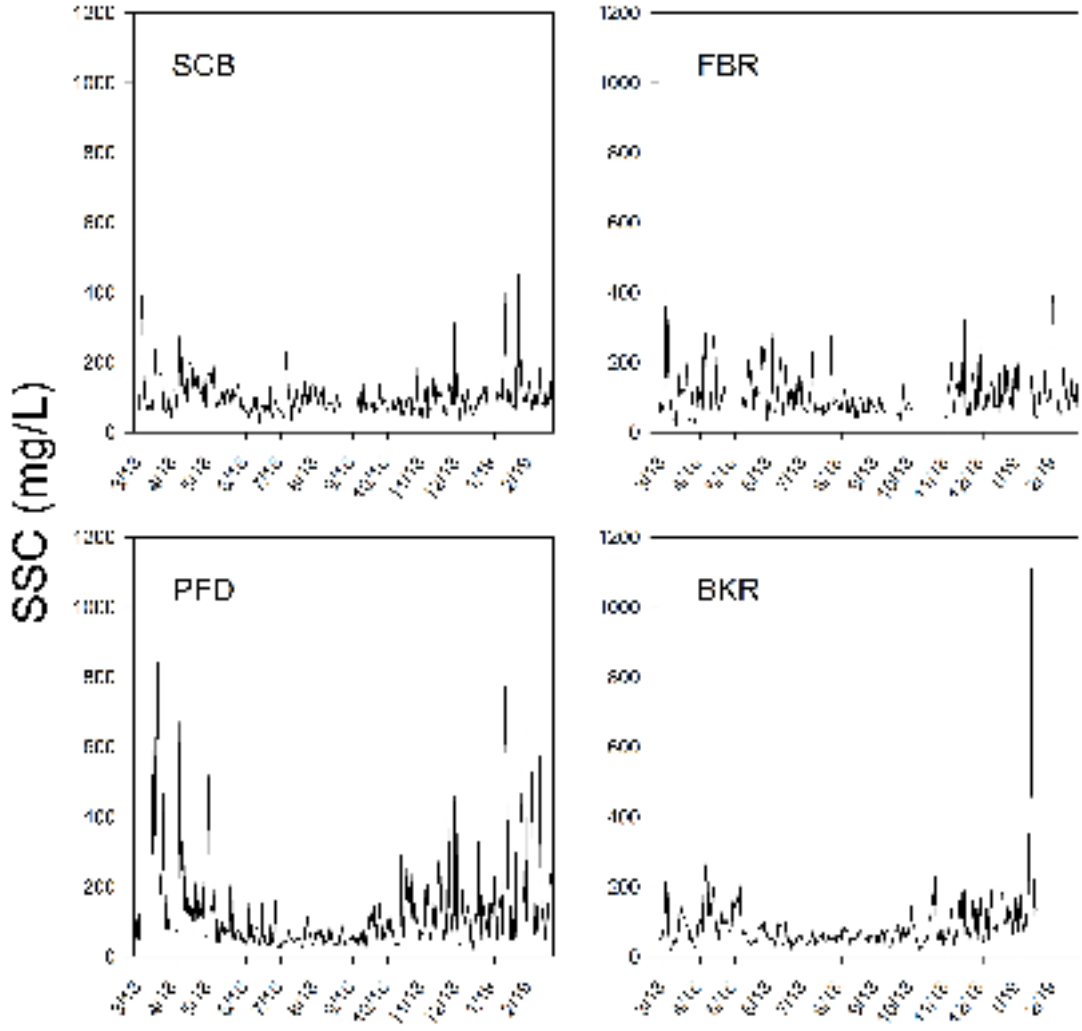

Figure 9. Time series of SSC from 2/24/2018 to 2/21/2019 at each station.

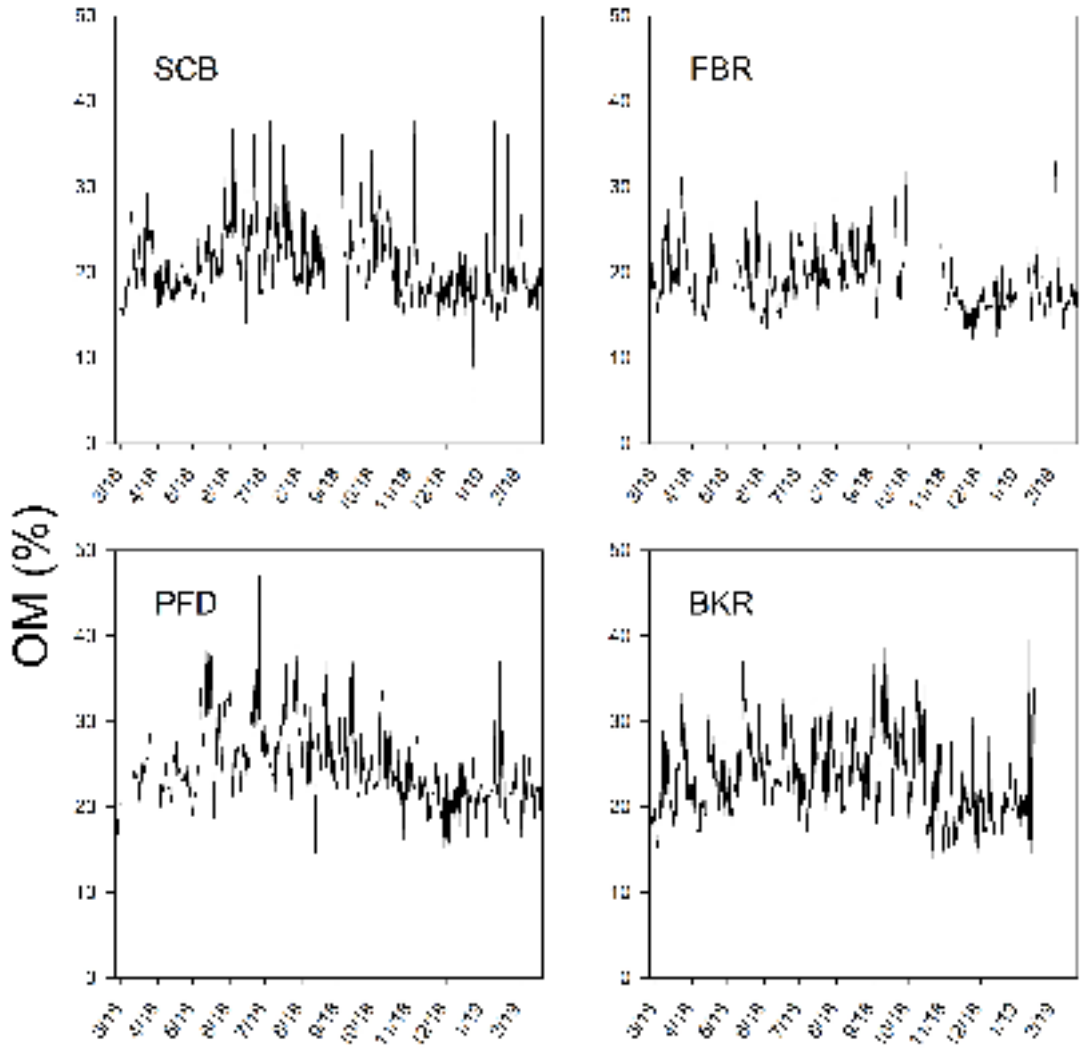

Figure 10. Time series of organic matter from 2/24/2018 to 2/21/2019 at each station.

By plotting SSC and OM as monthly averages, a seasonal trend is evident. These trends are presented in Figures 11 (SSC), 12 (OM by percentage), and 13 (OM by concentration) as box-and-whisker plots. SSC is significantly higher in the winter and lower in the summer as tested by a Wilcoxon signed rank test ($p < 0.001$; Figure 11). OM by percentage exhibits a significant opposite trend in Figure 12, being lower

in the winter and higher in summer ($p < 0.001$). Due to the higher average SSC in the winter, OM by concentration is also significantly higher in the winter than in the summer ($p < 0.001$; Figure 13). SSCs throughout the project show a larger range and higher median during the winter months.

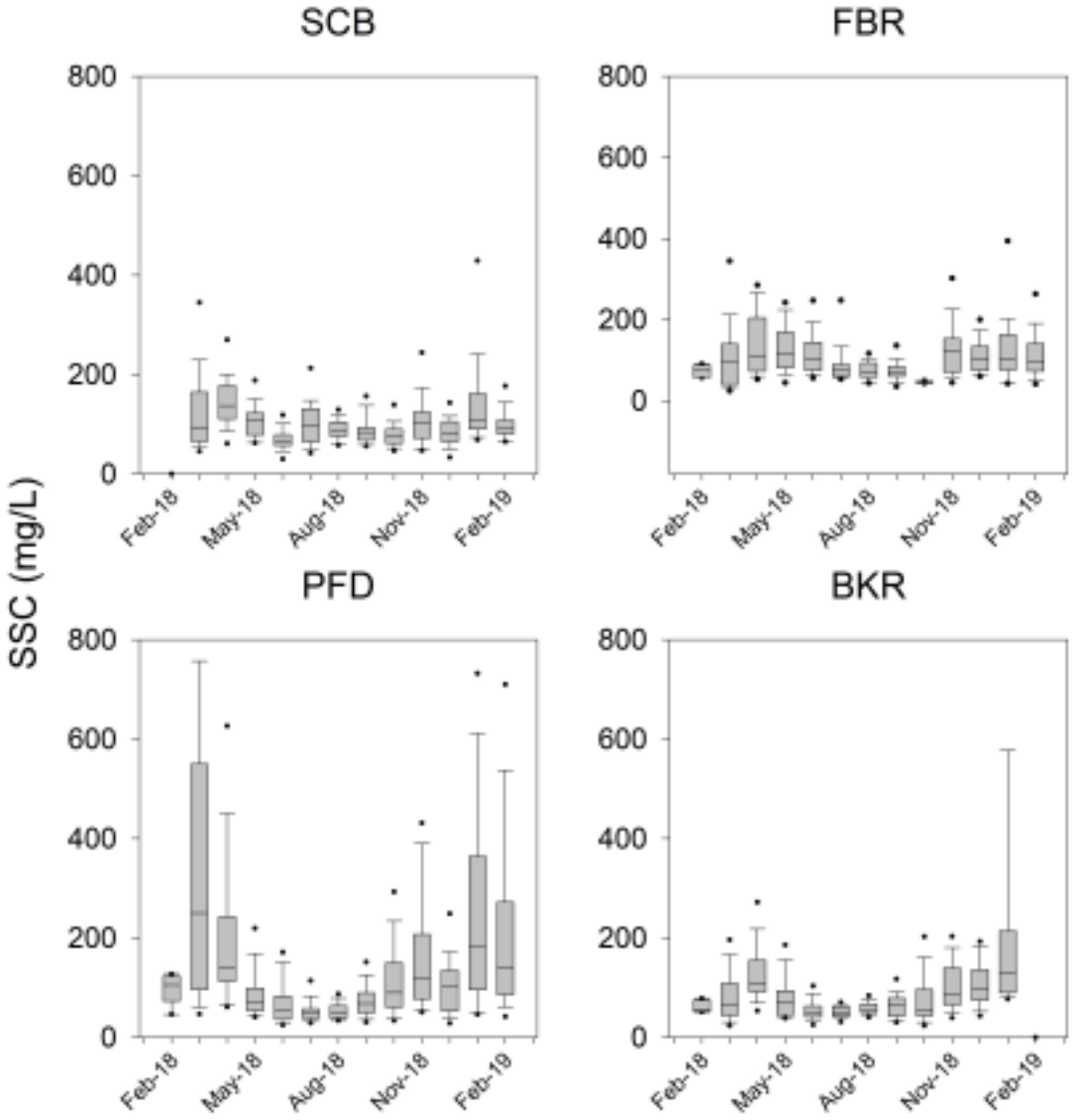

Figure 11. Monthly average SSC at each station. SSC was higher during the winter months than in the summer months.

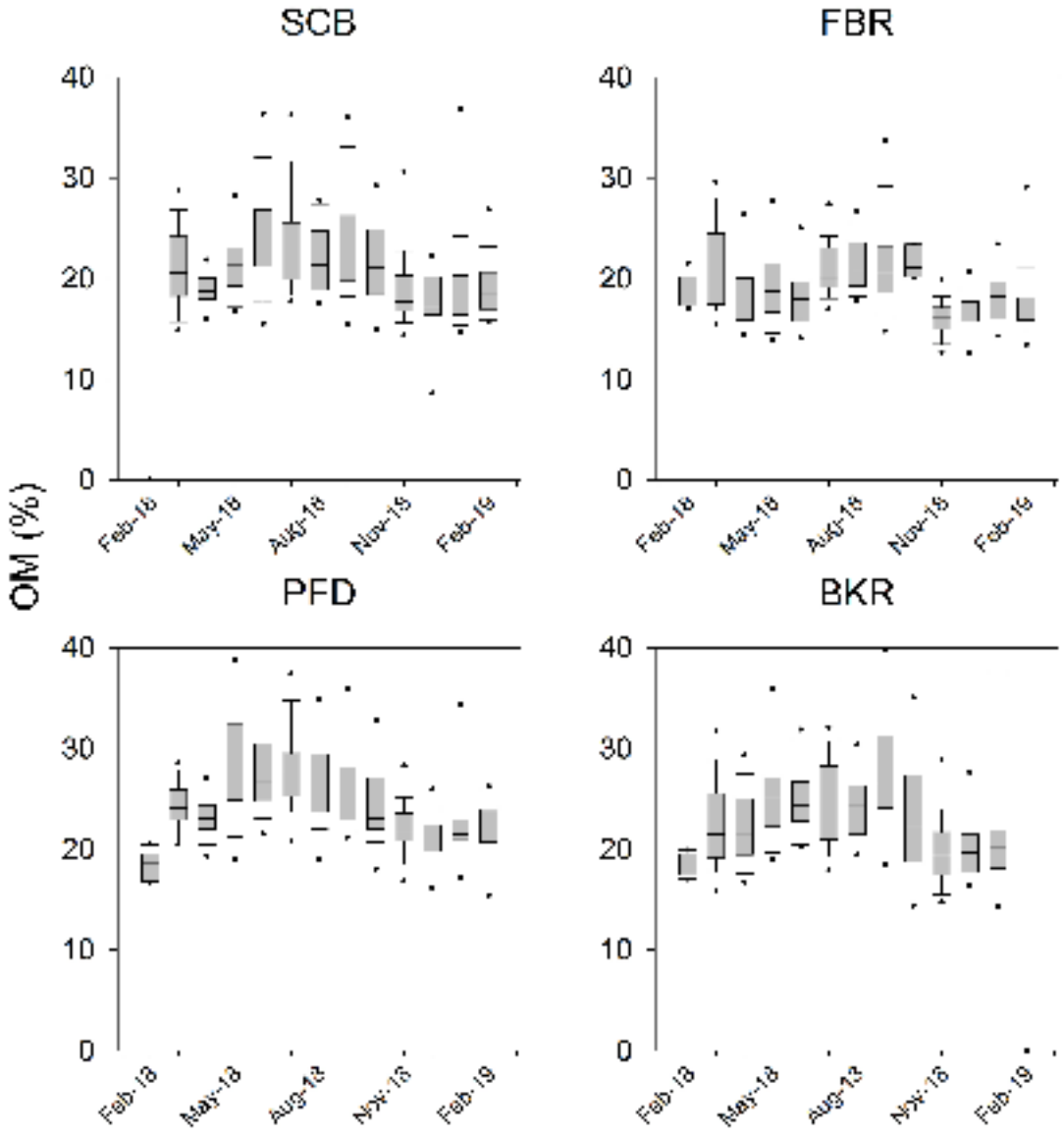

Figure 12. Monthly average OM by percent at each station. OM by percent was higher during the summer months than the winter months.

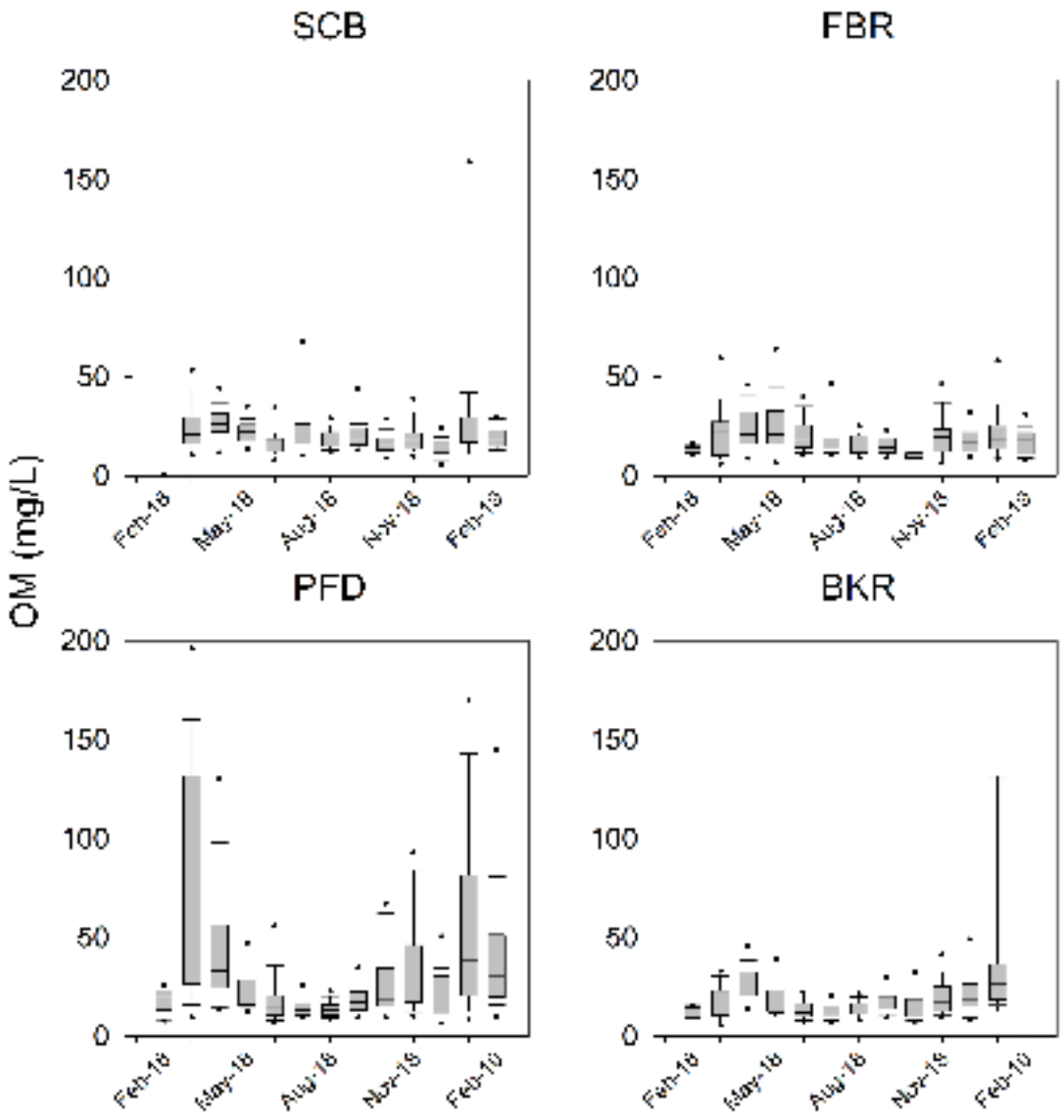

Figure 13. Monthly average OM by concentration at each station. OM by concentration was higher during the winter months than the summer months.

Figure 14 shows boxplots of SSC and OM, arranged similarly to Figure 2. Mean SSCs are listed in Table 4. Median SSC by station ranged from 68 to 91 mg/L. The SSC was, on average, highest at the SCB station and lowest at the BKR station. The maximum individual SSC measurement was 1108 mg/L at BKR. Each station had a minimum SSC value between 20 mg/L and 25 mg/L (Table 4). The standard error of SSC samples was 1.7 mg/L (2.3%).

Median values of OM ranged from 19% to 25%. Average OM was significantly higher at the two southern stations (PFD and BKR) than at the two northern stations (SCB and FBR) as tested by a Wilcoxon signed rank test ($p < 0.001$). The highest OM measurement was 47.2% at the PFD station and the lowest was 5.3% at SCB. Organic material from these sediments is primarily composed of living and dead algal material and marsh plant detritus. The numbers of daily observations for each station are listed in Table 3.

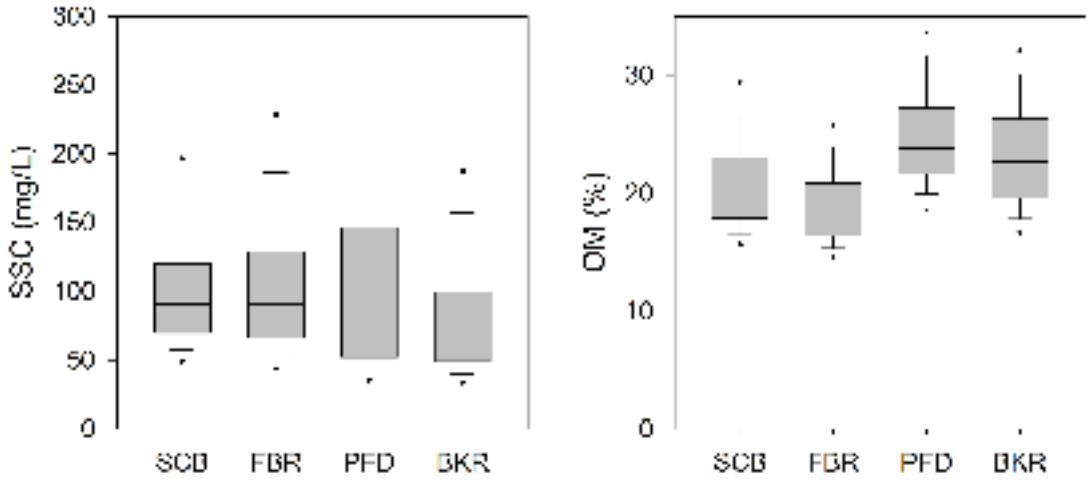

Figure 14. Boxplots of median SSC and OM at each station. SSC and OM at stations within the northern half of the refuge (Units I & II, SCB and FBR) are generally more similar to each other than those in the southern half (Units III & IV, PFD and BKR) and vice versa.

SSC and OM percentage throughout the study stations generally exhibit an inverse relationship ($r = -0.30$, $p < 0.001$); for example, as shown by samples from station BKR from March 1, 2018 to May 31, 2018 in Figure 15 ($r = -0.67$). Samples with higher SSCs had a lower percentage of organic material (Figure 15). One possible interpretation of this result is that, as SSC increased with resuspension of bed materials, organic material adsorbed on channel bed particles entered the water column. Because the OM content of organic material on the channel bed is generally lower than that in the water column (because of decomposition), resuspension events "dilute" the water-column OM and give rise to lower OM concentrations.

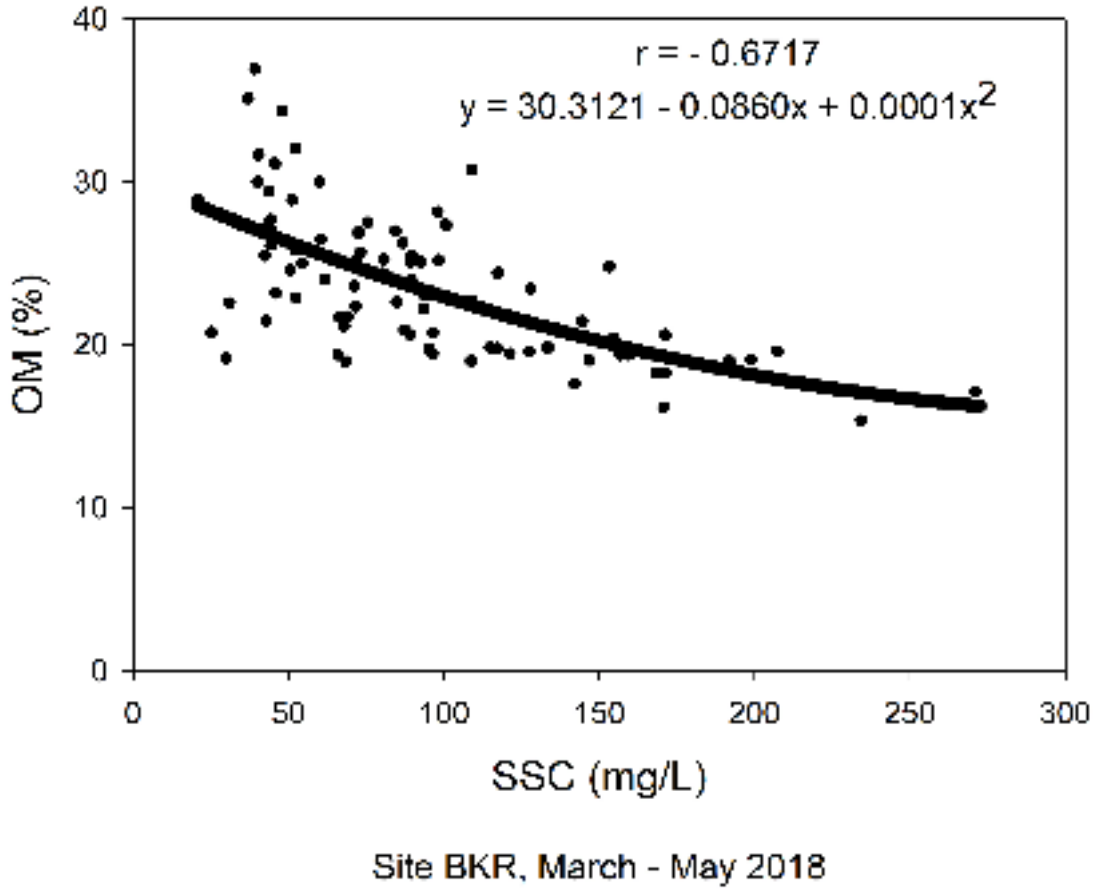

Figure 15. SSC and OM at station BKR from March - May 2018, showing a negative relationship between the two variables.

3.2.2 Correlation Among Refuge Stations

There was some correlation of daily SSC between the northern (SCB and FBR) and southern stations (PFD and BKR), suggesting that sediment flux in the refuge is spatially variable. However, other correlations across the north/south divide suggest the refuge acted more similarly as a whole. Pearson correlation coefficients of SSC between stations are listed in Table 5. The two northern and two southern stations

exhibited somewhat strong relationships with correlation coefficients of 0.64 and 0.75, respectively. When compared to a station in the other half of the refuge, the correlation coefficient was smaller than when compared to the neighboring station with the exception of SCB and BKR, which have a correlation coefficient of 0.67. P-values indicate that each relationship is significant, meaning that the refuge as a whole acted similarly in terms of SSC.

Table 5. Pearson correlation coefficients between SSC at each station. Each relationship was significant at $\alpha = 0.001$.

Station	SCB	FBR	PFD	BKR
SCB	1.0			
FBR	0.64	1.0		
PFD	0.28	0.37	1.0	
BKR	0.67	0.42	0.75	1.0

3.3 Sediment Flux

Daily sediment flux is shown by the column plots in Figure 16. Mineral sediment is represented by the black portion of the column and organic material by the red portion. The average sediment flux ranged from 23.8 g/s at station SCB to 61.8 g/s at station PFD as exports. The largest daily average sediment flux reached 3227 g/s as an export at PFD on 10 January 2019, while the largest sediment flux as an import amounted to 2015 g/s on 9 September 2018 at SCB.

Cumulative sediment flux (mineral plus organic portion) is illustrated in Figure 16 via the line plot and secondary y-axis. In Figure 16 for both daily and cumulative sediment flux, positive represents an export and negative represents an import. At each station, a net export of sediment was observed. Table 6 lists the net export over the period of study, reported as an annual rate in metric tons. The sum of these fluxes is

5,296 ± 112 metric tons/year (note: FBR, PFD, and BKR only are used in the sum to avoid double-counting as SCB occupies the same channel as FBR). The largest export of sediment occurred at the PFD station, followed by BKR. As there is little movement of water and interaction between Units II and III, flux measurements at each station can help describe sediment flux among refuge units. The cumulative sediment fluxes measured at the SCB and FBR stations were similar when considering the error associated with the fluxes, suggesting that there may be no net sediment transport between the two stations in Unit I. The net export of sediment measured at the FBR station indicates that material is exported from Unit II through Unit I, and out of the refuge. The sum of the sediment fluxes from PFD and BKR indicate the export from Unit III into Unit IV and beyond.

Utilizing the organic fraction of the sediment flux, a cumulative carbon flux can be calculated in a similar fashion as the cumulative sediment flux. A relationship between organic carbon and organic matter (through Loss-On-Ignition) was established by Craft et al. (1991) and can be calculated as:

$OC = 0.4 * LOI + 0.0025 * LOI^2$

where OC = organic carbon (%) and LOI = organic matter through loss-on-ignition (%).

These fluxes are listed in Table 6; the sum of the cumulative organic carbon flux for the FBR, PFD, and BKR stations (excluding SCB for double-counting purposes) was an export of 513 ± 12 metric tons/year, or about 10% of the total cumulative sediment flux. This study did not determine labile vs. recalcitrant carbon and the potential for decomposition, so this export is a maximum estimate.

The daily sediment flux in Figure 16 highlights the importance of capturing storm events to accurately characterize the cumulative flux as these events are often the cause of the large fluxes in either import or export direction. Unfortunately, equipment failures occurred throughout the study period at each station and limited our ability to describe all sediment flux events throughout the study period.

Table 6 lists a comparison of sediment import and exports. Sediment exports were more frequent than imports, ranging from 127 days (54% of total time) at station PFD to 217 days of export (75%) at station FBR.

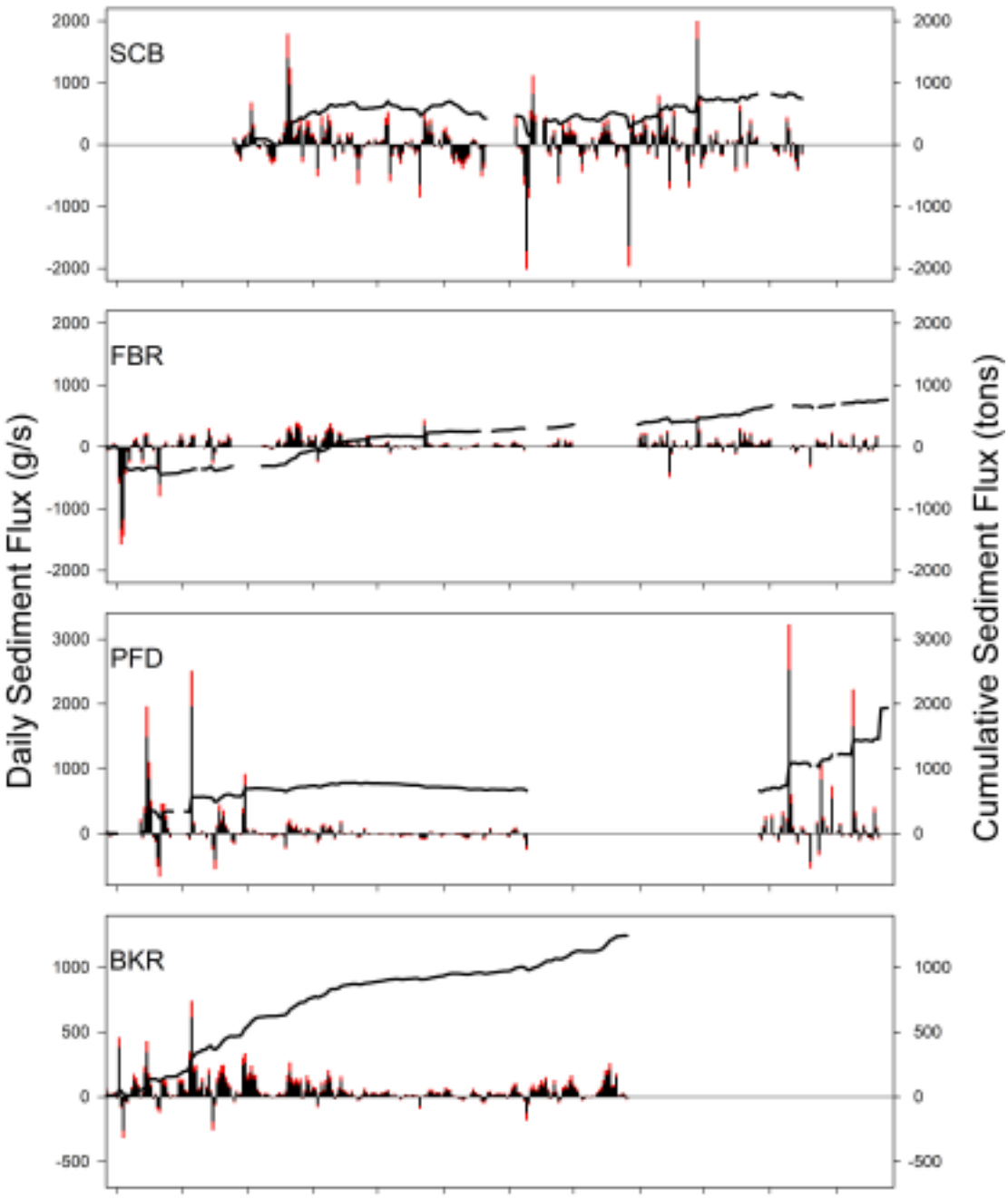

Figure 16. Daily sediment flux at each of the stations, reported in grams/second as both mineral and organic fractions as columns. Cumulative sediment flux is shown with a line plot on the secondary y-axis. In each y-axis, positive values represent and export of sediment from the system while negative values represent an import. Note the varying scales of the y-axes

Table 6. Cumulative sediment and carbon fluxes at each station, reported in metric tons/year, total count of days measured, and counts of days recording imports and exports.

Station	Sediment Flux (tons/year)	Carbon Flux (tons/year)	Total Daily Flux Measurements	Count of Import Days	Count of Export Days
SCB	1021 ± 134	153 ± 11	245	107	138
FBR	1179 ± 41	98 ± 4	289	72	217
PFD	2265 ± 30	235 ± 4	236	109	127
BKR	1852 ± 41	180 ± 4	245	46	199

3.4 Influence of Tide, Wind, and Precipitation

3.4.1 Meteorological Data

As a part of the analysis of the meteorological forcing mechanisms on sediment flux in the refuge, meteorological data were inspected and compared to the records of sediment flux. Daily averaged onshore wind speed averaged 2.1 m/s with a standard deviation of 1.1 m/s during the sampling period and reached a maximum on 3 March 2018 of 6.5 m/s. The winter exhibited significantly higher wind speed than the summer as per a Wilcoxon signed rank test ($p < 0.001$). The wind predominantly blew from the east-northeast, south-southwest, and west directions. When wind speed was high (average wind speed was greater than one standard deviation above the mean), the wind mostly blew from westerly directions (west, south-southwest, west-northwest, and north-northwest). Daily averaged offshore wind speed, measured at the Brandywine Shoal Light NOAA buoy in the Delaware Bay, was higher than that inland, at 7.1 m/s. There was precipitation recorded on 135 days, or 37.3% of the 362-day study period; the total precipitation was 134.1 cm or a rate of 135.2 cm/year. This amount of precipitation is higher than the annual average precipitation of 114 cm for

southern Delaware, thus this study took place during a slightly wetter year than the usual (Delaware Climate Information 2019).

3.4.2 Storm Events

Over the study period, 84 days exhibited either an onshore wind speed or a precipitation total that was greater than one standard deviation above the mean. This is equivalent to 23% of the days within the sampling period. For the purpose of this study, such events are considered storm events. This threshold was equivalent to a daily averaged wind speed of 3.2 m/s and daily precipitation total of 1.3 cm. Of these 84 days classified as storm events, 81 days overlapped with existing sediment flux data, and 13 days reached the threshold for both wind and precipitation. A total of 55 of the 81 events (68%) corresponded to an export of sediment from the refuge. The sediment flux on days of these storm events accounted for 20% of the total cumulative sediment flux, or 1,010 metric tons/year of the total calculated flux of 5,296 metric tons/year.

3.4.3 Correlation Analysis

Pearson's Correlation Coefficient tests were performed to determine the relative influence of tide, wind, and precipitation on SSC and water discharge. These tests measured both the direction and magnitude of relationships between these forcing mechanisms and factors of sediment flux in order to determine if variations in SSC or discharge can be attributed to tide, precipitation, or wind. A larger correlation coefficient represents a stronger relationship. Daily averaged water level was used as a proxy for tides, and daily averaged wind speed was used for wind. Precipitation was analyzed using daily total rainfall. Given the transient nature of meteorological forcing

mechanisms and low resolution of data (daily SSC), it is assumed that daily measurements of discharge, SSC, water level, wind, and precipitation measurements within their respective time series are independent.

Onshore wind speed, measured as a daily average at the University of Delaware station, was significantly positively correlated with SSC at each station, as shown in Table 7. Offshore wind speed was generally significantly positively correlated as well, but had a weaker effect than onshore wind. Precipitation was negatively correlated with SSC at each station except FBR, but significance is only established at the BKR. Water level was significantly negatively correlated with SSC at each station, indicating that resuspension is more likely to occur in shallow water. Water velocity was not significantly correlated with SSC, potentially highlighting a disconnect between the station positions (channels) and the area of SSC generation (flats). SSC was most strongly affected by onshore wind speed at all stations.

Discharge was strongly influenced by both offshore wind and water level (Table 8). This analysis was conducted using the absolute value of discharge to determine what mechanisms move water rather than which import or export water. At three of the four stations (SCB, FBR, PFD) offshore wind speed was significantly positively correlated with discharge. All four stations exhibited a significant positive correlation with water level. Tides most strongly influenced discharge, but wind significantly affected discharge at most sites.

Table 7. Pearson correlation coefficients of SSC and wind speed, precipitation, and water level by station.

SSC Station	Onshore Wind Correlation Coef.	Offshore Wind Correlation Coef.	Precipitation Correlation Coef.	Water Level Correlation Coef
SCB	0.3719***	0.1988*	-0.0031	-0.2826***
FBR	0.3272**	0.2709*	0.0166	-0.2096**
PFD	0.2308**	0.3726***	-0.0955	-0.1283*
BKR	0.4401***	0.2014	-0.1798**	-0.3164***

Significance codes: * 0.05, ** 0.01, *** 0.001

Table 8. Pearson correlation coefficients of the absolute value of discharge and wind speed, precipitation, and water level by station.

Discharge Station	Onshore Wind Correlation Coef.	Offshore Wind Correlation Coef	Precipitation Correlation Coef.	Water Level Correlation Coef
SCB	-0.0652	0.2474**	-0.2441***	0.4598***
FBR	0.1970	0.4140***	-0.0436	0.2175***
PFD	-0.1102	0.4169***	-0.0384	0.4374***
BKR	0.2687*	0.01835	-0.0711	0.4074***

Significance codes: * 0.05, ** 0.01, *** 0.001

A cross-correlation function at each station between precipitation and discharge shows a lag between a significant effect where precipitation significantly positively affects discharge between one and five days after it occurs, as plotted at a Lag of -1 to -5 (Figure 17). In Figure 17, each vertical line stemming from the zero reference line on the y-axis represents the autocorrelation function (ACF) measurement of the lag, which, in this application, corresponds to one day. Significance is noted when the autocorrelation coefficient measurement exceeds the

blue dotted line, at an ACF of about -0.105 and 0.105. A table of autocorrelation coefficients is available in Appendix A. This lag can be attributed to the time required for precipitation to travel from the watershed to the refuge via surface runoff and groundwater flow. Discharge is not significantly affected by precipitation on the day precipitation occurs, but is significantly affected as early as one (SCB & PFD) and as late as five (SCB & BKR) days after precipitation occurs. The cross-correlation coefficients of precipitation and discharge are generally closer to zero than the correlation coefficients of wind with the exception of SCB, suggesting that wind is a stronger driver of discharge than precipitation.

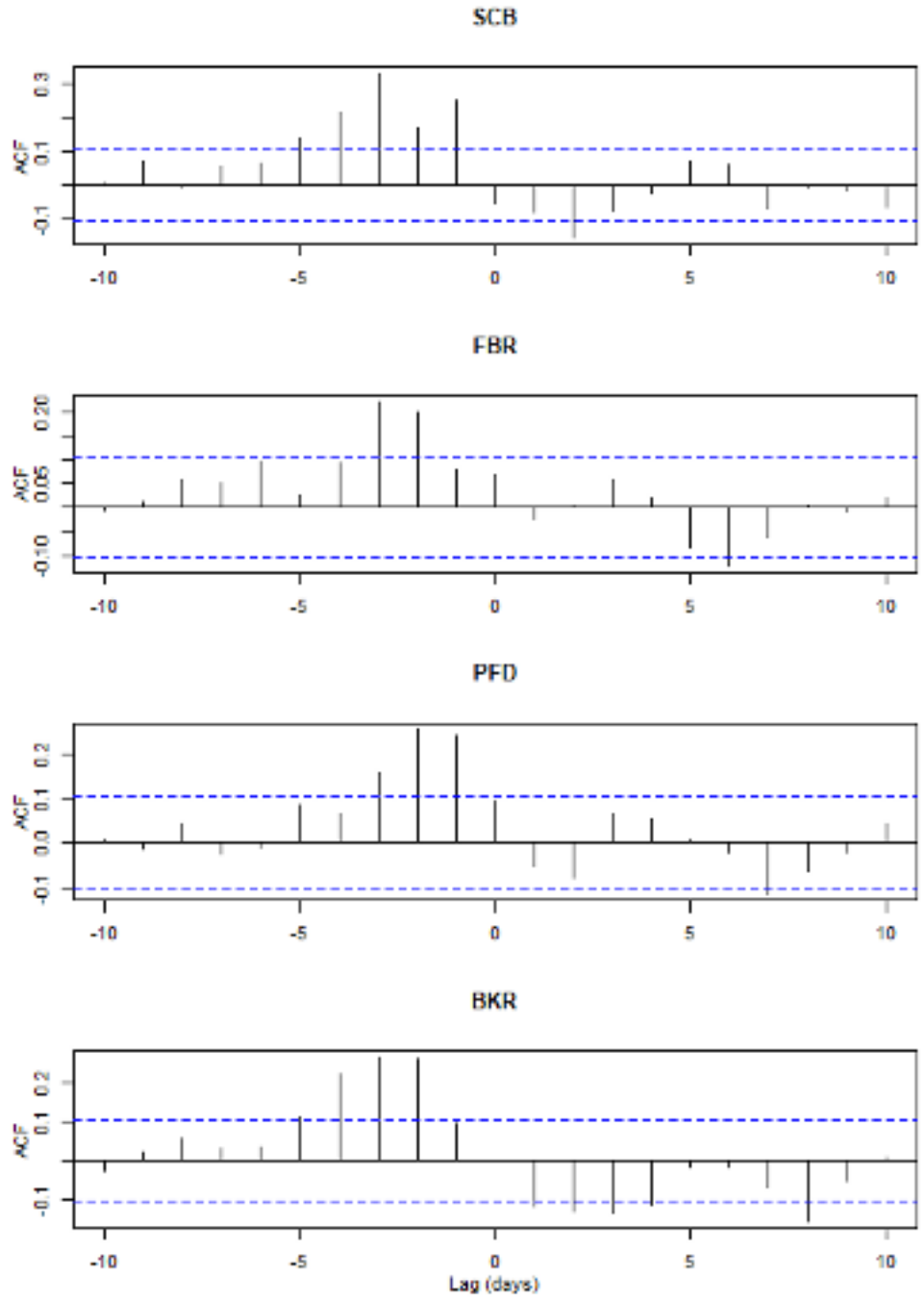

Figure 17. Cross Correlation Function plots for precipitation and discharge at each station. Precipitation and discharge were positively correlated at a lag of -1 to -5 days.

Results indicate that wind speed is the predominant forcing mechanism on temporal variation in SSC. As wind speed increases, SSC increases as well. Water level significantly affects SSC as well, with a lower water level correlated with higher SSC. Because much of the refuge is open water with a large fetch, wind waves that develop resuspend bed sediments, particularly when there is tide water over the flats. This suggests the water regime of the refuge is affected by both tide and wind forces, but that the sediment regime is wind-dominated because of wave resuspension. Evidence of this resuspension is present when analyzing the relationship between SSC and organic content (Figure 15). In addition to sediment from the flats, other sediment sources include channel bank erosion and surface runoff from upland areas.

While there was no significant correlation between precipitation and discharge occurring on the same day, a lag between the two is apparent as shown in Figure 17. Discharge events are positively correlated with precipitation events within one to five days prior. It is intuitive that surface runoff and groundwater flow from Prime Hook Creek and Slaughter Creek to the refuge increases during rainstorms, thus increasing discharge at the monitoring stations.

Sediment flux is most strongly influenced by SSC at each station due to the large SSC variability (standard deviation among stations ranges from 54 to 134 mg/L). Through examining the data, SSC may account for most of the flux variance, but large sediment flux events require both a high SSC and discharge, whether it be import or export.

3.5 Frequency Analysis

A power spectral density analysis was conducted to determine the effect of the spring-neap tidal cycle on the daily averaged velocity and SSC at each station in the

refuge. The largest spectrum peaks in Figures 18 and 19 refers to the strongest periodicity of the velocity and SSC at each station, respectively. The red dotted line in Figures 18 and 19 indicates the frequency of 0.03389, or 1/29.5. The reciprocal of this frequency defines the period of the lunar month or spring-neap tidal cycle of 29.5 days.

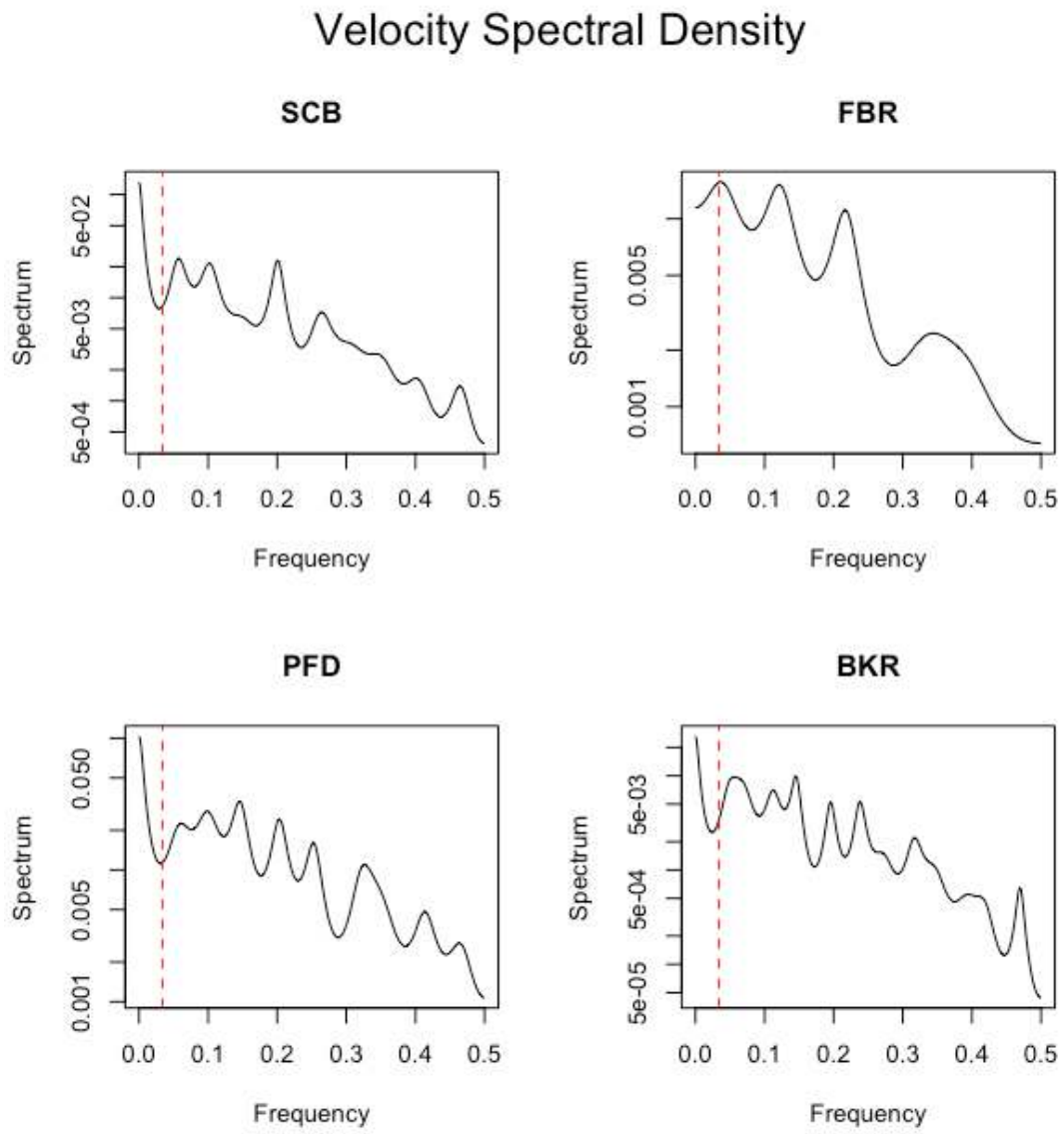

Figure 18. Periodograms of daily averaged velocity for each station in the refuge. Peaks in the spectrum describe the periodicity of velocity. The red dotted line labels the period of the spring-neap tidal cycle. The data are smoothed through an autoregressive model.

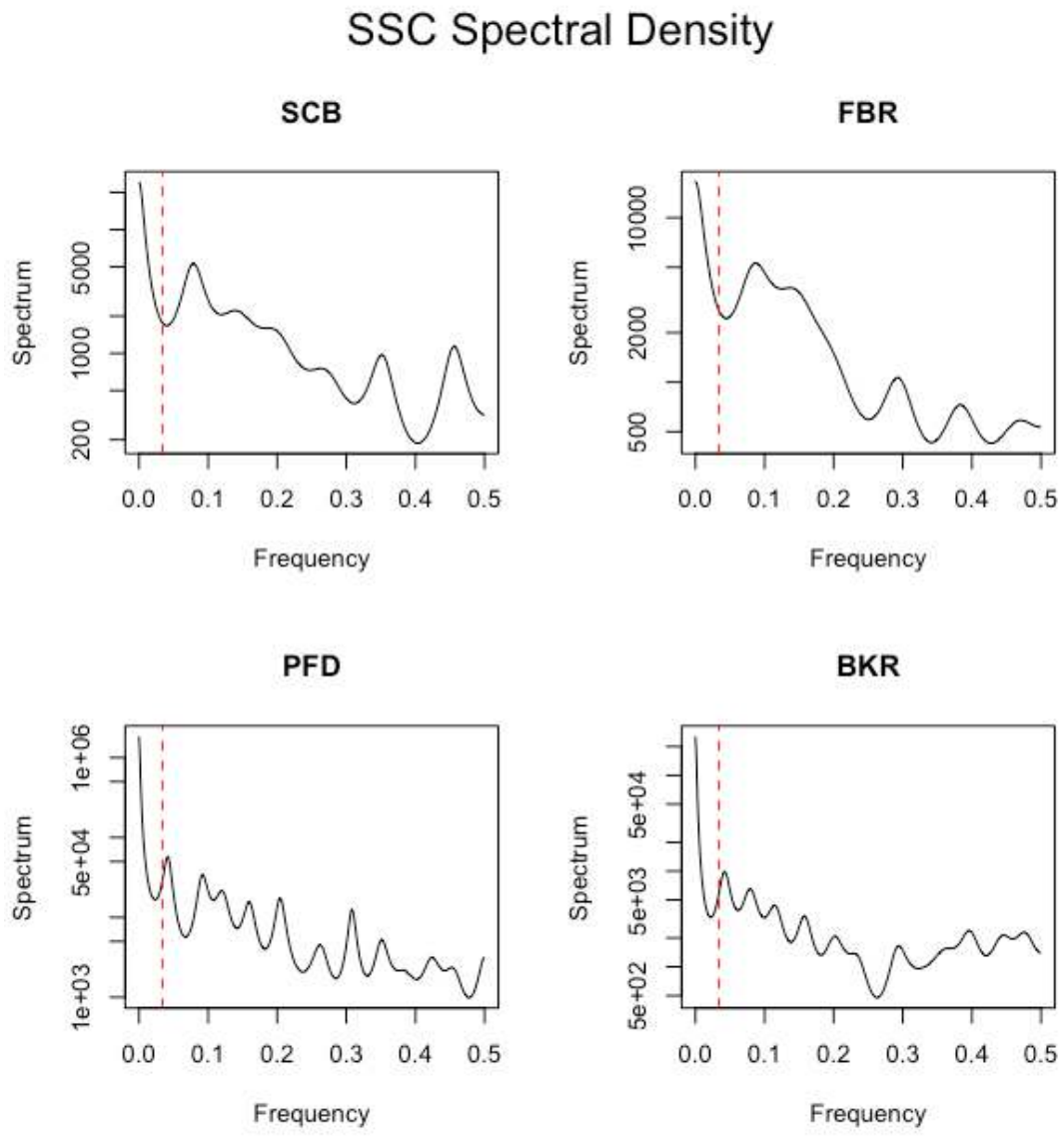

Figure 19. Periodograms of SSC for each station in the refuge. Peaks in the spectrum describe the periodicity of velocity. The red dotted line labels the period of the spring-neap tidal cycle. The data are smoothed through an autoregressive model.

Table 9. Period in days of the largest spectrum peak for velocity and SSC.

	Period (days)	
Station	Velocity	SSC
SCB	17.5	12.8
FBR	28.5	11.5
PFD	6.9	24.4
BKR	25.0	23.8

As listed in Table 9, the strongest period frequency of velocity only closely matches the spring-neap cycle (29.5 days) at the FBR station, and the strongest period frequency of SSC does not match the spring-neap cycle at any station in the refuge. The variance in the largest spectrum peak and misalignment with the period of the spring-neap cycle show that the water velocity and SSC within the refuge exhibit a weak periodicity and random effects are strongly influential.

3.6 Transport Events

Storm events, characterized by a combination of storm surge, local winds, and precipitation, are apparent in the data during the period of this study. This section will describe the storm characteristics of two major events and present data for each monitoring station. Events in July and November 2018 were selected based on the large magnitude of the measured sediment flux. The July event illustrates a storm surge, and the November event demonstrates a blow-out tide.

In Figures 20 through 25, data plots are organized with daily averaged wind speed (line) and daily precipitation (bar) on top. The wind direction is listed at the scale of secondary intercardinal directions beneath the wind speed and precipitation plot. Below that, daily SSC is shown as a line plot. Water level relative to NAVD88 and discharge are plotted with the instantaneous as the thick black line and low-passed as the thin grey line. Finally, sediment flux is shown last. Negative discharge and

sediment flux values represent an import while positive values represent an export of water or sediment. A gray dotted line is plotted at zero in the discharge and sediment flux plots to visually differentiate between export and import.

3.6.1 July Event

Event summaries by station for the July 2018 event are presented in Figures 20-23. In this timeframe, an import event occurred around the 21st, and an export event followed around the 23rd. Wind speed was moderate but consistent on the 21st through 24th, and direction changed from northerly and easterly from the 19th through 21st to southerly from the 22nd through 25th. On July 21, 2018, over 5 cm of precipitation fell at the nearby Lewes meteorological station.

Increased flood tide amplitude on the 21st and northerly and easterly winds on the 19th through 21st pushed water from the Delaware Bay into the mouths of the Mispillion and Broadkill Rivers. Water levels throughout the stations generally increased following the precipitation event on the 21st and, along with the southerly winds, dropped over the following days.

SSC varied among stations but generally was high around the 21st; this date typically corresponded with the sediment flux peak for the July event. As the water level rose from wind and precipitation, water was imported at each station on the 21st or 22nd. At SCB, PFD, and BKR, this input of water and sufficiently high SSC caused an import of sediment. On July 21st, all stations imported sediment totaling 89 metric tons. The majority of this import (74 tons) took place at SCB.

After the 22nd, water levels fell from southerly winds acting as a blowout tide and drainage of rainfall, causing a net export of water. SSC was again sufficiently high and peaks at the FBR and PFD stations. A net positive discharge was seen at the SCB,

FBR, and BKR stations, leading to exports of sediment. Between the 23rd and 27th, about 225 metric tons of sediment were exported from the system. Again, sediment flux at SCB was most extreme among stations, with 100 metric tons of export in that period.

In the second event (23rd through 27th), the two northern stations (SCB and FBR) behaved similarly; both exhibited a larger range of water level and discharge compared to their average and had a peak export of sediment on the 23rd. The two southern stations behaved similarly as well: small net sediment fluxes stemmed from mostly low SSC and small discharges.

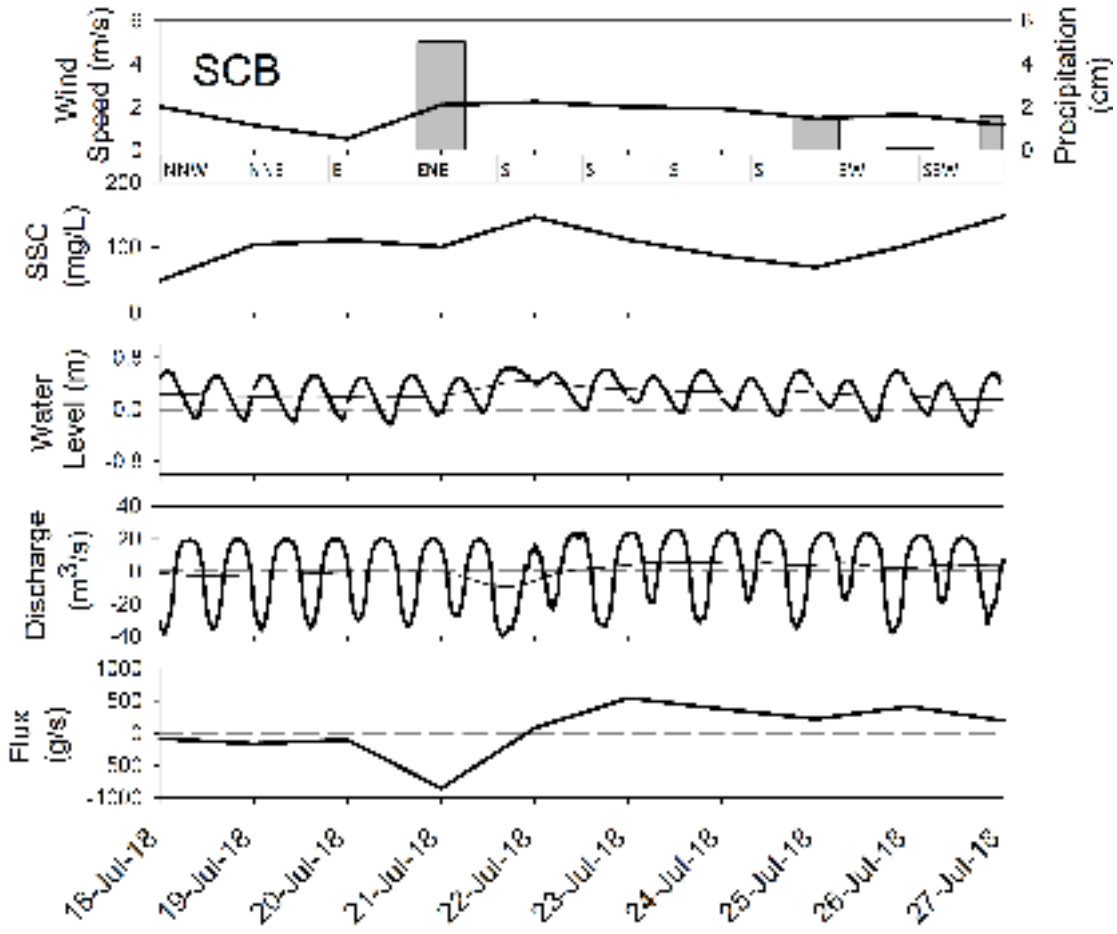

Figure 20. Wind speed and direction, precipitation, SSC, water level, discharge, and sediment flux from 18 to 27 July 2018 at SCB.

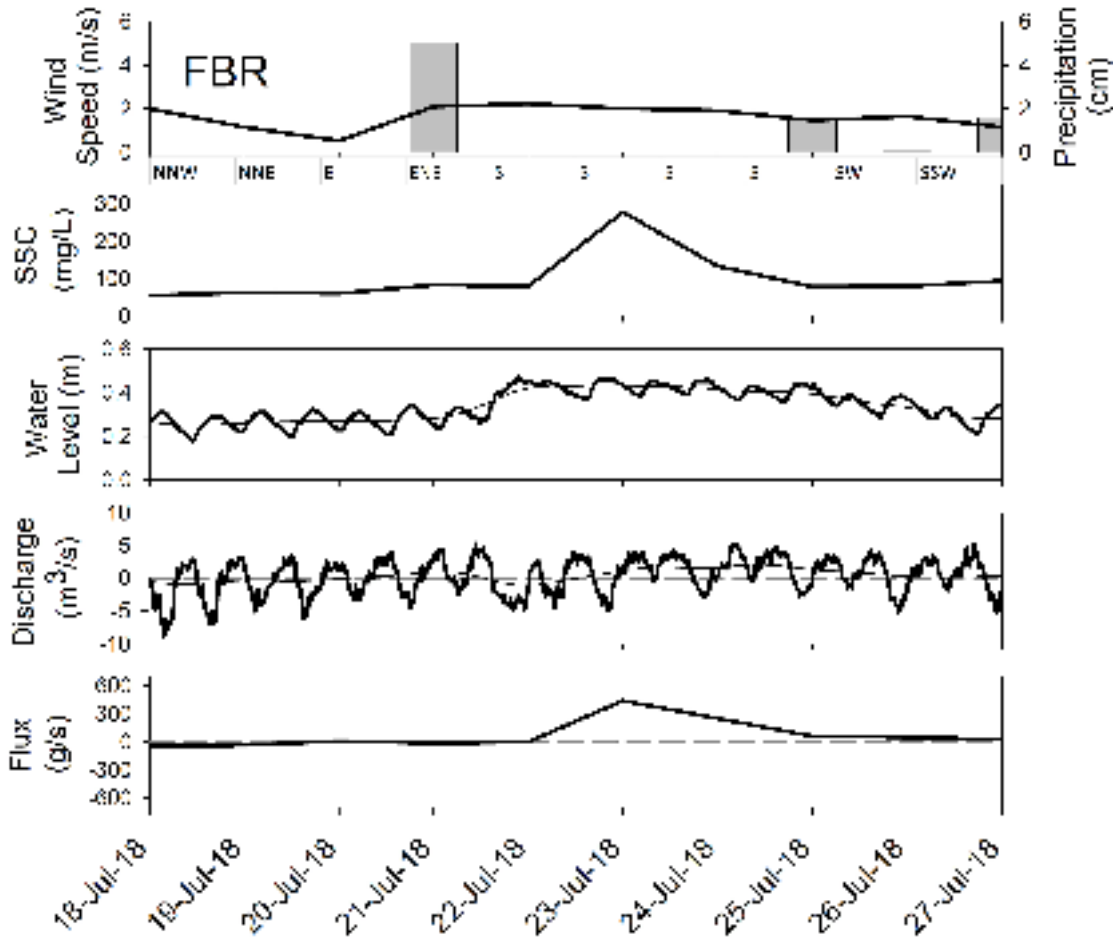

Figure 21. Wind speed and direction, precipitation, SSC, water level, discharge, and sediment flux from 18 to 27 July 2018 at FBR.

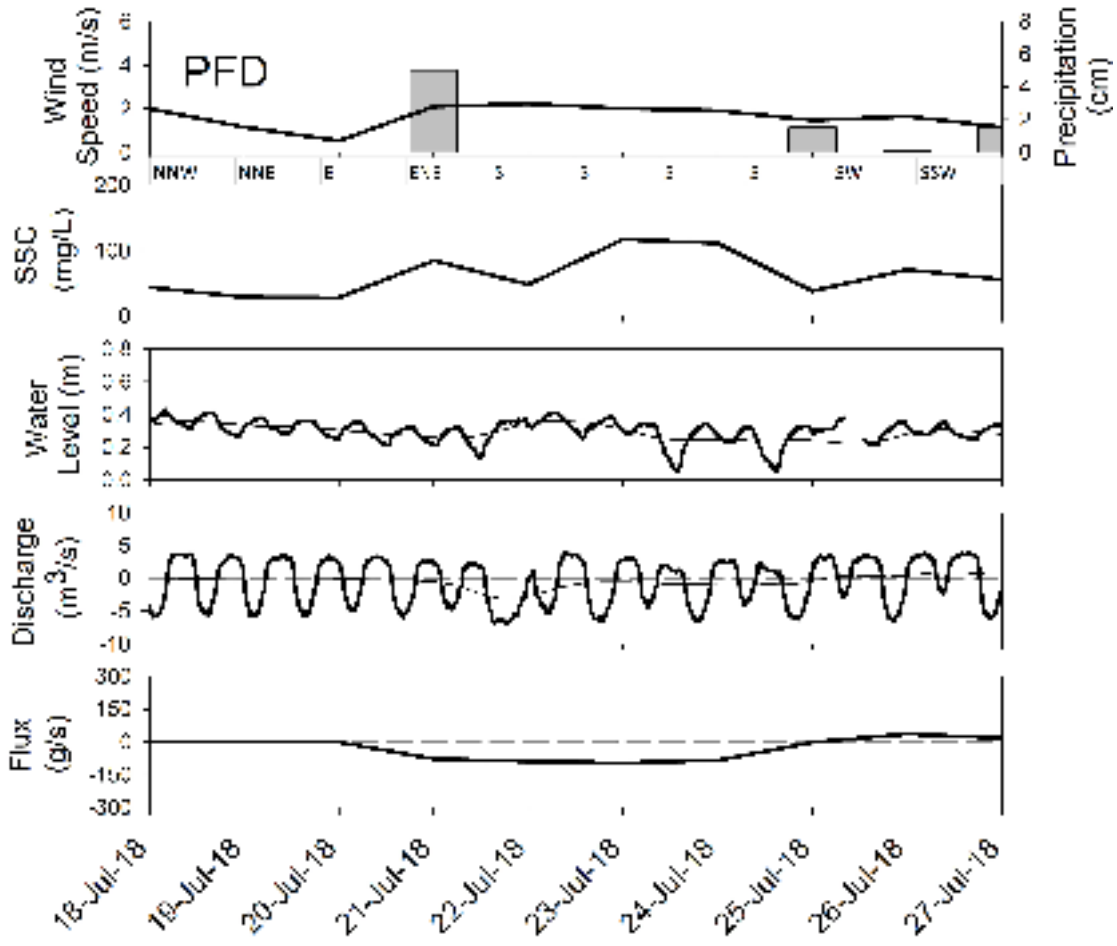

Figure 22. Wind speed and direction, precipitation, SSC, water level, discharge, and sediment flux from 18 to 27 July 2018 at PFD.

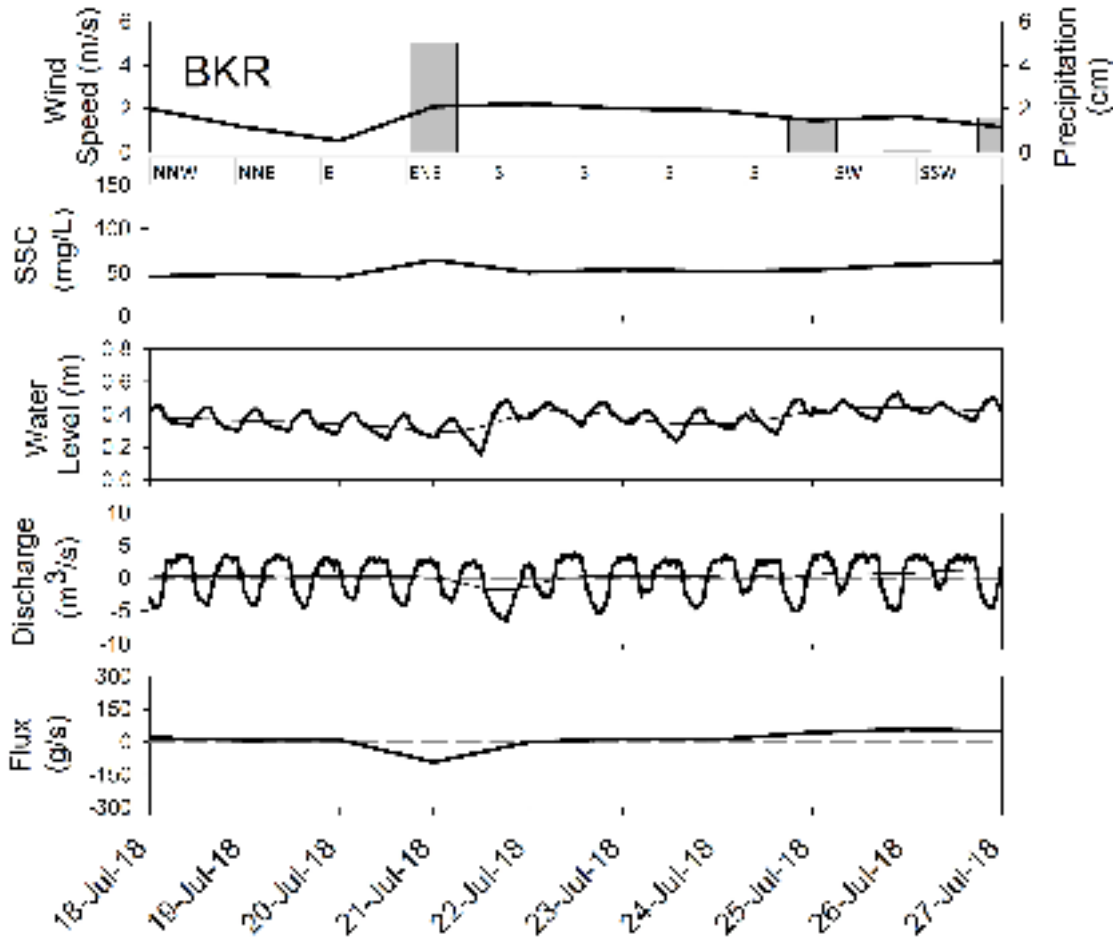

Figure 23. Wind speed and direction, precipitation, SSC, water level, discharge, and sediment flux from 18 to 27 July 2018 at BKR.

3.6.2 November Event

A strong wind event occurred between 27 and 29 November 2018, during which the average daily wind speed was over one standard deviation above the mean wind speed for the study period. Data for the SCB and FBR stations are shown below in Figures 24-25 (PFD and BKR data for this time period are incomplete due to ADP malfunctions).

The strong winds on the 27th through 29th corresponded with high SSC at all observed stations. A blowout tide caused by wind from the west and west-northwest direction pushed water out of the refuge to the Delaware Bay. Water levels dropped at each station around the 28th, causing a net export of water (positive discharge). High water and sediment levels leaving the refuge combined to create a net flux of sediment out of the refuge, visible at each station on the 28th. Between the 27th and 29th, over 307 metric tons of sediment were exported from the system. The flux at station SCB accounted for 262 tons of sediment.

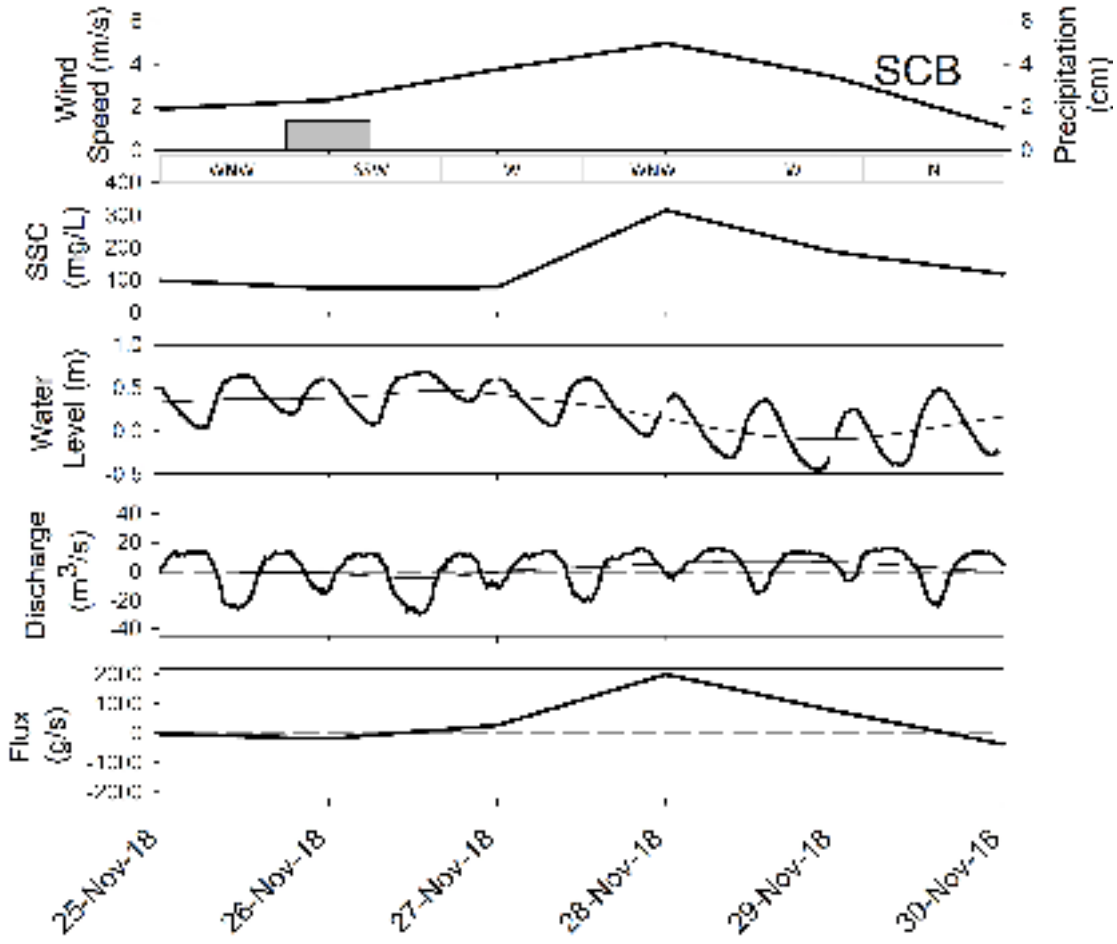

Figure 24. Wind speed and direction, precipitation, SSC, water level, discharge, and sediment flux from 25 to 30 November 2018 at SCB.

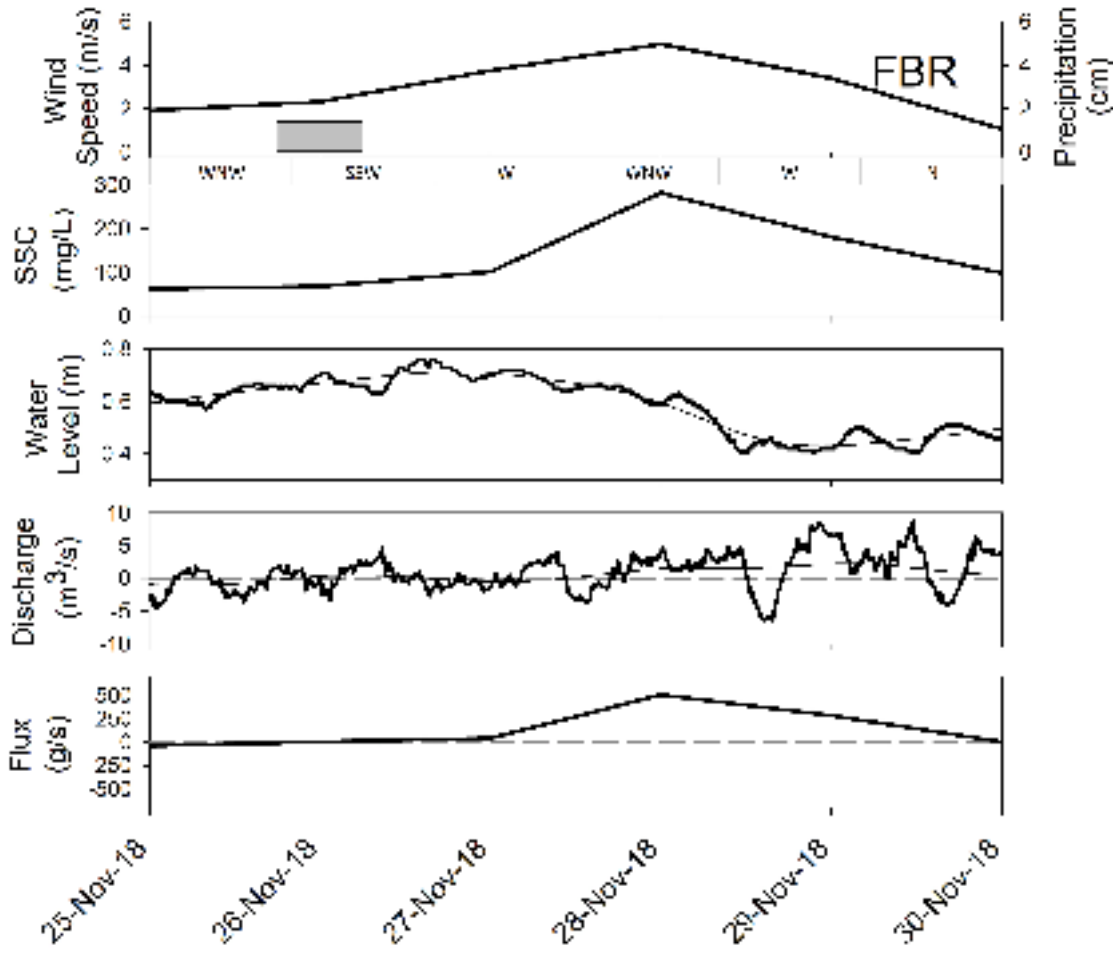

Figure 25. Wind speed and direction, precipitation, SSC, water level, discharge, and sediment flux from 25 to 30 November 2018 at FBR.

Chapter 4

DISCUSSION

Through the study period of 24 February 2018 to 21 February 2019, a mean discharge of water out of the refuge caused suspended sediment from the marsh to be exported. The mean water discharge out of the refuge is prominent in examining the velocity, water level, and finally discharge measurements. SSC is generally high and is positively correlated with onshore wind speed. Storms influence water flow and may cause discharge over event timescales to either import or export water, based on the nature of the storm (level of precipitation and direction and intensity of wind).

4.1 Sediment Flux Comparison

Based on the mean water discharge out of the refuge and high SSC, this study found a cumulative export of sediment from the refuge to the Delaware Bay estimated at 5,296 ± 112 metric tons/yr. To put this flux into perspective, historical sediment loading estimates are available for the Broadkill and Mispillion Rivers from a 1974 USGS study by Mansue and Commings (1974). That study estimated that each river exported 499 metric tons of sediment annually (Mansue and Commings 1974). Our findings represent sediment loading from the refuge, which includes tributaries to the Broadkill and Mispillion Rivers. Other tributaries to these rivers exist but were not sampled in our study; the refuge contributes just a portion of the total water discharge and sediment loading to the Broadkill and Mispillion Rivers. Current export rates of sediment flux of the refuge are several times larger than the combined sediment loading (export) of the Broadkill and Mispillion Rivers estimated by Mansue and Commings in 1974.

4.2 Refuge Erosion

Another way to give context to the total sediment flux from the refuge is to express it as an estimated net rate of erosion from the refuge units. This derived net erosion rate assumes a uniform rate over the area of the channels and open water in the refuge, though in reality erosion is spatially variable. The total area comprising of channel and open water makes up approximately 1470 acres of the wetland complex according to GIS analysis. The erosion rate can be calculated by dividing the rate of total sediment flux (g/yr) by the range of bulk density of the sediment (g/cm^3) and further dividing by the total area (cm^2). Bulk density of the refuge sediment in Units II and III was previously measured by Boyd and Sommerfield (2016) as 0.33 g/cm^3 to 1.26 g/cm^3. Given this range of bulk density, the range of erosion rates value 0.07 cm/yr to 0.27 cm/yr. This strictly considers the suspended sediment transport and does not take other aspects of elevation loss or gain into account, such as subsidence or peat development.

Ganju et al. (2015) provides an erosion rate in terms of weight of sediment per unit area of 0.56 $kg/m^2/yr$ in the nearby Blackwater River, MD (2015). This study's measured sediment flux of 5,296 tons/yr converts to 0.87 $kg/m^2/yr$ based on dividing the annual flux rate by the total channel and open water area (1470 acres). The Blackwater River, Ganju et al. (2015) note, is also a wind-dominated system and has undergone disturbance from invasive rodents and shoreline erosion. Given the large manipulation of sediments during the Prime Hook restoration, an erosion rate 1.5x that of the Blackwater River is not unreasonable. A review by Stevenson et al. (1988) suggests the net sediment flux from high salinity marshes along the mid-Atlantic coast represents an export of 1 to 2 $kg/m^2/yr$, which closely matches results from the present study.

4.3 Conceptual Sediment Flux Model

A conceptual model of sediment flux at the refuge can be developed based on the present observations. During this study period, the refuge exhibited a net export of sediment. Various forcing mechanisms can combine to create extreme sediment flux events that significantly influence the annual sediment budget; these events were seen to both import and export sediment on different occasions. An inspection of the time series of data resulted in four general sediment flux conditions that dominated the record and which inform the conceptual sediment transport model: fair weather, storm surge, northeast winds, and southwest winds. These sediment flux conditions are described below and illustrated in Figures 26 and 27. In those figures, larger arrows depict the forcing mechanism described. For simplicity in the diagram, in Figure 27 "Northeast Winds" refers to wind from the north or east and "Southwest Winds" refers to wind from the south or west. The effect of the wind direction on sediment flux is strongest when the wind direction travels from the two combined listed directions.

In fair weather conditions, the ebb dominance of water flow in the system leads to a net export of sediment as illustrated in Figure 26. These conditions are associated with low wind speeds and regular tidal action. Freshwater runoff leads to a net export of water (Figures 2 and 7), which carries fine-grained sediment with it out of the refuge. A high proportion of unvegetated wetland acreage in the refuge contributed to generally high SSC (~100 mg/L) even during fair weather conditions, as supported by Ganju et al. (2015). Without vegetation, the substrate is more easily eroded from a lack of physical structure. Plant stems can trap sediment (French and Spencer 1993) and reduce flow velocity (Petticrew and Kalff 1992) while vegetative belowground biomass can contribute to substrate stability (Redfield 1972).

The storm surge category refers to events where a measured water level surge event in the Delaware Bay contributed to high water levels and an import of water in the refuge. These events are driven by winds on the continental shelf, driving energy towards the coast. Storm surge events contributed to imports of water sediment as the flood tide increased in magnitude, carrying additional sediment into the refuge with the opportunity for settling (Figure 26). Wind speeds during storm surge events are often high, but the Storm Surge diagram in Figure 26 depicts only water and sediment flux due to the storm surge. Further effects of wind are presented in Figure 27.

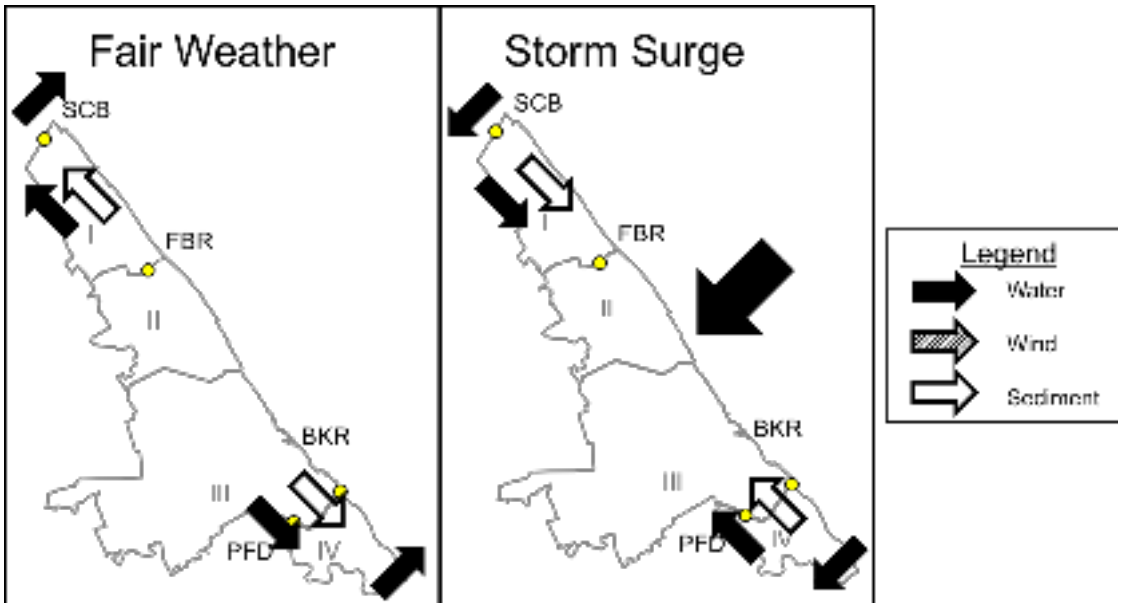

Figure 26. Conceptual diagram depicting directional flow of water and sediment flux in fair weather conditions and during storm surges. The monitoring stations are depicted by the yellow circles.

Northerly and easterly winds typically pushed water from the Delaware Bay towards the refuge, resulting in a small increase in water level near the coast and

inside the refuge. This build-up of water continues into the mouths of the Broadkill and Mispillion river and further into the refuge. As this water flows from the Delaware Bay into the refuge, it carries sediment with it, resulting in an import of material. This is depicted by "Northeast Winds" in Figure 27.

Winds from the south and west directions caused a blowout tide, where water was pushed from the refuge into the Delaware Bay, lowering water levels. Exports of material occurred during these events, titled "Southwest Winds" in Figure 27. Combining wind speed with direction can help predict how the refuge will react to a meteorological event. During the study period, strong winds typically blew from the west, northwest, and southwest. Consequently, there was a general export of suspended sediment from the refuge.

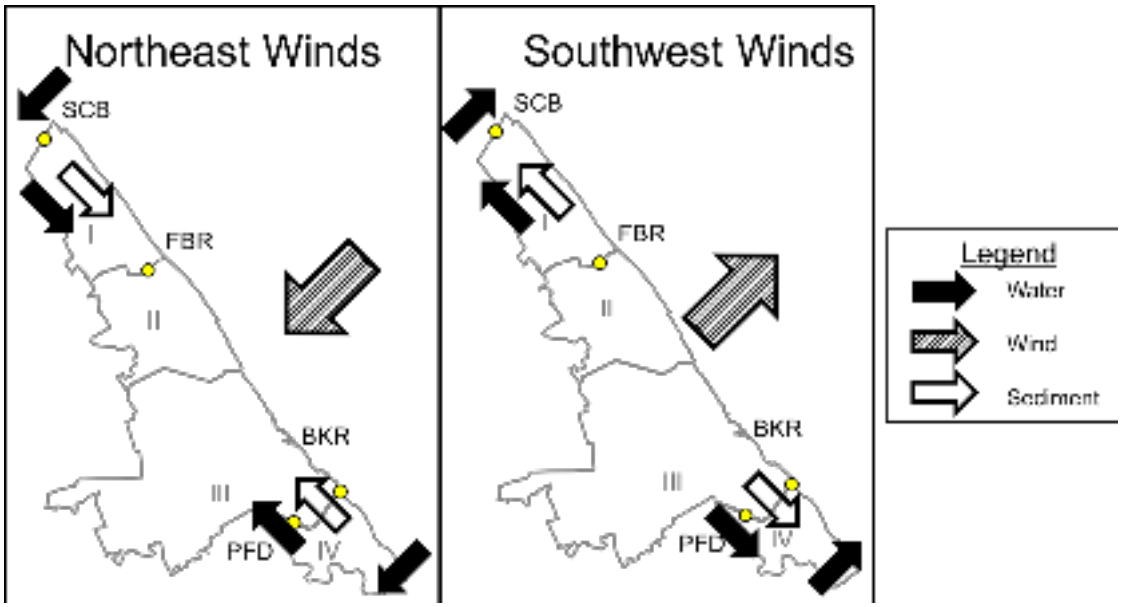

Figure 27. Conceptual diagram depicting directional flow of water, wind, and sediment flux in during periods of northeast and southwest winds. The monitoring stations are depicted by the yellow circles.

Precipitation did affect water discharge, though the effect came after a one to five-day lag, with the strongest effect occurring two and three days after the precipitation event (Figure 17). Apparently, groundwater and surface runoff from rainfall can reach the tidal creeks after one to five days and influence discharge. This influx of water from the land contributes to the ebb-dominance of the system and can drive water and sediment out of the refuge. If wind speed is sufficient after a precipitation event, and particularly if the wind blows from the south or west, these two mechanisms may combine to create a major sediment export event.

The July import event described in 3.6.1, which occurred from July 19th through the 21st was indicative of a storm surge. Northeast winds and incoming energy from a storm pushed water towards the refuge and produced precipitation, creating a net import of water and sediment. This build-up of water then slowly drained from the refuge, aided by southerly winds, and a net export of water and sediment is experienced in the following July event. The November event in section 3.6.2 demonstrated a blow-out tide. High winds from the west caused a high SSC and pushed water out of the tidal inlets of the refuge and drain towards the Delaware Bay, exporting both sediment and water.

This study reinforces examples in the literature of wind-dominated systems based on local weather patterns and morphology (Janssen-Stelder 2000, French et al. 2008, Allen and Duffy 1998) and the finding that storms can either import or export sediment (Pethick 1992). An example from the literature that motivated a portion of this study's hypothesis, Ganju et al. (2015) stating the relationship between vegetative cover and sediment flux was also supported.

4.4 Future Considerations

A key aspect of climate change is the expected increase in coastal storm frequency and intensity (Scavia et al. 2002). In this section, net flux refers to the actual measured flux from the refuge (exports – imports) while gross flux refers to the total sediment flux (exports + imports). During this study period, storms generated about 20% of the net sediment flux while storm event days totaled 23% of the study period. On the whole, the net sediment transport during storm events was similar to that during fair weather conditions. When considering individual events, the sediment transport during storm events was larger; the net effect of storms was diminished as the events contained both imports and exports of sediment. Of the gross sediment flux, storms accounted for 44%. The net flux during fair weather and storm days are similar, at 5.6 and 5.9 metric tons/day (export), respectively, but when considering the gross flux, the rates increase to 8.4 and 16.7 metric tons/day, respectively. In the future, the effect of storms on the net sediment flux is likely to become more dominant with an expected increase of storm frequency and intensity (Scavia et al. 2002). Though storm characteristics and patterns may change to preferentially import or export sediment in the future, it is reasonable to assume that they will continue to act to both deposit and erode sediment in the refuge. If changes in climate led to more northeast wind conditions, typical of nor'easter storms, the sediment imports to the refuge may increase. Conversely, if the frequency of blowout tides via southerly and westerly winds increase, a more extreme export of sediment may be experienced. Considering sea level rise, storms of lower intensity may also be able to significantly move sediment in the future. An increase in storm frequency or intensity could lead to the system being more episodic and event-driven.

Given the efforts to revegetate the area during the restoration project and removal of water impoundment systems, the trend of sediment export measured in this study is expected to decrease in magnitude or reverse to be an import, potentially allowing the accretion rate to match that of relative sea level rise. A duplication of this study after the system has stabilized following the 2016 restoration could more clearly answer if marsh accretion can match relative sea level rise.

Chapter 5

CONCLUSION

The Prime Hook National Wildlife Refuge in Milton, Delaware recently underwent an extensive restoration effort following damage from Hurricane Sandy to stabilize about 4,000 acres of marsh habitat, in order to improve the resilience of the refuge in the face of the increasing frequency of coastal storms and sea level rise. This study aimed to understand sediment flux dynamics in the refuge following the restoration, with a working hypothesis stating that the refuge as a whole would export sediment due to a large percentage of unvegetated area.

By continuously measuring water flow and sediment characteristics at four stations within the refuge from February 2018 to February 2019, an annual sediment flux for the refuge could be calculated and seasonal effects examined. By analyzing meteorological data, sediment flux forcing mechanisms were identified and a conceptual sediment flux model was developed.

Two small freshwater creeks caused a net export of water from the refuge. Suspended sediment concentrations (SSC) were high on average (~100 mg/L) compared to natural marshes in the area (10-40 mg/L). SSC consisted of about 20% organic matter. During the winter, SSC was significantly higher and wind speed significantly faster than during the summer, leading to larger sediment fluxes. Through a correlation analysis, it was found that wind speed has the largest influence on SSC of parameters measured. Wind speed and tidal action together drive the discharge of water, with precipitation having a significant but lesser effect one to five days after discharge events. Freshwater runoff leads to a net export of water, which carries fine-grained sediment with it out of the system. The spring-neap tidal cycle did not

significantly affect SSC or net discharge. Storm surge and northeast winds caused an import of sediment while southwest winds caused an export; storms tended to export sediment more often than they imported. The net sediment flux from the refuge was an export of 5,296 ± 112 metric tons/yr. Based on this finding, the working hypothesis that the refuge would export sediment could not be rejected.

Storms accounted for 20% of the net flux but 44% of the gross flux, indicating that they are not the dominant mechanism but have a high potential for sediment transport considering climate change projections predict an increase in storm intensity and frequency. Given the size of the refuge and recent disturbances from storms and the restoration activity, this total export is relatively small and comparable to values in the literature of similar ecosystems.

This study did not address bedload sediment flux or measures of accretion including organic matter production. Given that the vegetative cover of the wetland is continuing to increase following the restoration effort, this susepended sediment flux may decrease in magnitude or reverse to an import in the future; a replication of this study in the future as the wetland complex stabilizes would provide further insight into the effectiveness of the restoration project and the role of coastal marshes on partial exchange with adjacent estuaries.

REFERENCES

American Meteorological Society (AMS), 2000. Glossary of Meteorology, 2nd Edition. Boston: AMS, 850p. Retrieved from http://glossary.ametsoc.org/wiki/nor'easter

Allen, J. R. L., and Duffy, M. J. (1998). Medium-term sedimentation on high intertidal mudflats and salt marshes in the Severn Estuary, SW Britain: the role of wind and tide. *Marine Geology*, *150*(1), 1–27. Retrieved from https://doi.org/10.1016/S0025-3227(98)00051-6

The American Littoral Society (2012). *Assessing the Impacts of Hurricane Sandy on Coastal Habitats*. Retrieved from https://www.nfwf.org/hurricanesandy/Documents/Hurricane-Sandy-Coastal-Habitats.pdf

Aubrey, D. (1986). Hydrodynamic Controls on Sediment Transport in Well-Mixed Bays and Estuaries. In Physics of Shallow Estuaries and Bays, J. van de Kreeke (Ed.). Retrieved from https://doi.org/10.1029/LN016p0245

Boyd, B. M., Sommerfield, C. K. (2016). Marsh accretion and sediment accumulation in a managed tidal wetland complex of Delaware Bay. *Ecological Engineering, 92, 37-46.* https://doi.org/10.1016/j.ecoleng.2016.03.045

Chen, S.-L., Zhang, G.-A., Yang, S.-L., and Shi, J. Z. (2006). Temporal variations of fine suspended sediment concentration in the Changjiang River estuary and adjacent coastal waters, China. *Water Resources in Regional Development: The Okavango River*, *331*(1), 137–145. https://doi.org/10.1016/j.jhydrol.2006.05.013

Childers, D. L., and Day, J. W. (1990). Marsh-water column interactions in two Louisiana estuaries. I. Sediment dynamics. *Estuaries*, *13*(4), 393–403. https://doi.org/10.2307/1351784

Clarkson, B. R., Ausseil, A. G. E., and Gerbeaux, P. (2013). Wetland ecosystem services. *Ecosystem services in New Zealand: conditions and trends. Manaaki Whenua Press, Lincoln*, 192-202. http://www.landcareresearch.co.nz/__data/assets/pdf_file/0020/77042/1_14_Clarkson.pdf

Costanza, R., Groot, R., Sutton, P., Van der Ploeg, S. & Anderson, S., Kubiszewski, I., Farber, S., Turner, R. (2014). Changes in the global value of ecosystem services. Global Environmental Change. 26. 152–158. Retrieved from https://doi.org/10.1016/j.gloenvcha.2014.04.002

Craft, C. B., Seneca, E. D., & Broome, S. W. (1991). Loss on ignition and kjeldahl digestion for estimating organic carbon and total nitrogen in estuarine marsh soils: Calibration with dry combustion. *Estuaries*, *14*(2), 175–179. https://doi.org/10.2307/1351691

Dahl , T.E. 1990. *Wetlands Losses in the United States 1780's to 1980's.* U.S. Department of the Interior, Fish and Wildlife Service, Washington. D.C. 13pp. Retrieved from https://www.fws.gov/wetlands/documents/Wetlands-Losses-in-the-United-States-1780s-to-1980s.pdf

Dahl, T. E., Johnson, C. E., & Frayer, W. E. (1991). Wetlands, status and trends in the conterminous United States mid-1970's to mid-1980's. US Fish and Wildlife Service. Retrieved from http://hdl.handle.net/1969.3/24361

Davis, R., and Dolan, R. (1993). Nor'easters. *American Scientist*, 81(5), 428-439. Retrieved from http://www.jstor.org/stable/29775010

DeLaune, R.D., A. Jugsujinda, G.W. Peterson, and W.H. Patrick,. (2003). Impact of Mississippi River freshwater reintroduction on enhancing marsh accretionary processes in a Louisiana estuary, *Estuarine, Coastal and Shelf Science, Volume 58*, Issue 3, 2003, Pages 653-662, ISSN 0272-7714, https://doi.org/10.1016/S0272-7714(03)00177-X.

Delaware Climate Information. (2019). Office of the Delaware State Climatologist. University of Delaware. Retrieved from http://climate.udel.edu/delawares-climate

Delaware Department of Natural Resources and Environmental Control (2015). *2015-2025 Delaware Wildlife Action Plan*. Dover, Delaware, USA. Retrieved from http://www.dnrec.delaware.gov/fw/dwap/Pages/WAP-Progress.aspx

Deloffre, J., Lafite, R., Lesueur, P., Lesourd, S., Verney, R., and Guézennec, L. (2005). Sedimentary processes on an intertidal mudflat in the upper macrotidal Seine estuary, France. *Estuarine, Coastal and Shelf Science*, *64*(4), 710–720. https://doi.org/10.1016/j.ecss.2005.04.004

Downing-Kunz, M. A., and Schoellhamer, D. H. (2013). Seasonal variations in suspended-sediment dynamics in the tidal reach of an estuarine tributary. *Marine Geology*, *345*, 314-326. https://www.sciencedirect.com/science/article/pii/S0025322713000352

Dronkers, J. (1986). Tidal asymmetry and estuarine morphology. *Netherlands Journal of Sea Research*, *20*(2), 117–131. https://doi.org/10.1016/0077-7579(86)90036-0

Fagherazzi, S., Kirwan, M. L., Mudd, S. M., Guntenspergen, G. R., Temmerman, S., D'Alpaos, A., Clough, J. (2012). Numerical models of salt marsh evolution: Ecological, geomorphic, and climatic factors. *Reviews of Geophysics*, *50*(1). https://doi.org/10.1029/2011RG000359

French, J. R., Burningham, H., and Benson, T. (2008). Tidal and Meteorological Forcing of Suspended Sediment Flux in a Muddy Mesotidal Estuary. *Estuaries and Coasts*, *31*(5), 843. https://doi.org/10.1007/s12237-008-9072-5

French, J. R., and Spencer, T. (1993). Dynamics of sedimentation in a tide-dominated backbarrier salt marsh, Norfolk, UK. *Marine Geology*, *110*(3), 315–331. https://doi.org/10.1016/0025-3227(93)90091-9

Friedrichs, C. T. (1995). Stability Shear Stress and Equilibrium Cross-Sectional Geometry of Sheltered Tidal Channels. *Journal of Coastal Research*, *11*(4), 1062–1074. Retrieved from www.jstor.org/stable/4298411

Friedrichs, C. T. (2011). 3.06-Tidal Flat Morphodynamics: A Synthesis. *Virginia Institute of Marine Science: Gloucester Point, VA, USA*, 137-170. http://web.vims.edu/~cfried/cv/2011/Friedrichs_2011_Treatise.pdf

Friedrichs, C., and Perry, J. (2001). Tidal Salt Marsh Morphodynamics: A Synthesis. *Journal of Coastal Research,* 7-37. Retrieved from http://www.jstor.org/stable/25736162

Frostick, L. E., and McCave, I. N. (1979). Seasonal shifts of sediment within an estuary mediated by algal growth. *Estuarine and Coastal Marine Science*, *9*(5), 569–576. https://doi.org/10.1016/0302-3524(79)90080-X

Ganju N. K., Kirwan Matthew L., Dickhudt Patrick J., Guntenspergen Glenn R., Cahoon Donald R., and Kroeger Kevin D. (2015). Sediment transport-based metrics of wetland stability. *Geophysical Research Letters*, *42*(19), 7992–8000. https://doi.org/10.1002/2015GL065980

Ganju N. K., Nidzieko Nicholas J., and Kirwan Matthew L. (2013). Inferring tidal wetland stability from channel sediment fluxes: Observations and a conceptual model. *Journal of Geophysical Research: Earth Surface*, *118*(4), 2045–2058. https://doi.org/10.1002/jgrf.20143

Hutchinson S. E., Sklar, F., and Cindy Roberts. (1995). Short Term Sediment Dynamics in a Southeastern U.S.A. Spartina Marsh. *Journal of Coastal Research, 11*(2), 370-380. Retrieved from http://www.jstor.org/stable/4298346

Janssen-Stelder, B. (2000). The effect of different hydrodynamic conditions on the morphodynamics of a tidal mudflat in the Dutch Wadden Sea. *Continental Shelf Research*, *20*(12), 1461–1478. https://doi.org/10.1016/S0278-4343(00)00032-7

Johnston, C.A. (1994) Cumulative impacts to wetlands. *Wetlands. 14*: 49-55. https://doi.org/10.1007/BF03160621

Kirwan, M. L., Guntenspergen, G. R., D'Alpaos, A., Morris, J. T., Mudd, S. M., and Temmerman, S. (2010). Limits on the adaptability of coastal marshes to rising sea level. *Geophysical Research Letters*, *37*(23). https://doi.org/10.1029/2010GL045489

Kirwan, M. L., and Megonigal, J. P. (2013). Tidal wetland stability in the face of human impacts and sea-level rise. *Nature*, *504*, 53. https://doi.org/10.1038/nature12856

Laenen, A. and Curtis, Jr., R. E. (1989). Accuracy of acoustic velocity metering systems for measurement of low velocity in open channels. *U.S. Geological Survey Water-Resources Investigations Report 89-4090.* https://pubs.usgs.gov/wri/1989/4090/report.pdf

Leathers, D. 2019. *Delaware Climate Information.* Office of the State Climatologist. http://climate.udel.edu/delawares-climate

Letzsch W. S., R. W. Frey; (1980). Deposition and erosion in a Holocene salt marsh, Sapelo Island, Georgia. *Journal of Sedimentary Research*, *50* (2): 529–542. doi: https://doi.org/10.1306/212F7A45-2B24-11D7-8648000102C1865D

Levesque, V.A., and Oberg, K.A., 2012, Computing discharge using the index velocity method*: U.S. Geological Survey Techniques and Methods* 3–A23, 148 p. http://pubs.usgs.gov/tm/3a23/

Mansue, L. J., Commings, A. B. (1974). *Sediment Transport by Streams Draining into the Delaware Estuary*. US Geological Survey Water-Supply Paper 1532-H. Retrieved from https://pubs.usgs.gov/wsp/1532h/report.pdf

Marsh Restoration. (2018). U.S. Fish and Wildlife Service. Retrieved from https://www.fws.gov/refuge/Prime_Hook/what_we_do/marshrestoration.html

Moskalski, S. M., Sommerfield, C. K. (2013) Effects of Northeaster Storms on Water Level and Turbidity in a Delaware Bay Subestuary. Journal of Coastal Research: Volume 29, Issue 6a: pp. 205 – 213. https://doi.org/10.2112/JCOASTRES-D-12-00222.1

Moskalski, S. M., Torres, R. (2012). Influences of tides, weather, and discharge on suspended sediment concentration. *Continental Shelf Research: 37*, Pages 36-45. ISSN 0278-4343, https://doi.org/10.1016/j.csr.2012.01.015.

Nicholls, R. J. (2004). Coastal flooding and wetland loss in the 21st century: changes under the SRES climate and socio-economic scenarios. *Climate Change*, *14*(1), 69–86. https://doi.org/10.1016/j.gloenvcha.2003.10.007

NOAA (2019). *Lewes, DE – Station 8557380*. Tides and Currents. Retrieved from https://tidesandcurrents.noaa.gov/stationhome.html?id=8557380

Pethick, J. S. 1992. Saltmarsh Geomorphology. *In*: Allen, J. R. L., and Pye, K. (eds.), *Saltmarshes: Morphodynamics, Conservation, and Engineering Significance*. Cambridge University Press, U.K., 41-62.

Petticrew, E. L., Kalff, J. (1992). Water flow and clay retention in submerged macrophyte beds. *Canadian Journal of Fisheries and Aquatic Sciences*. Vol. 49, no. 12, pp. 2483-2489, 1992. Retrieved from: https://doi.org/10.1139/f92-274

Phillips, Jonathan D. (1989). Fluvial Sediment Storage in Wetlands. 1. *JAWRA Journal of the American Water Resources Association*, *25*(4), 867–873. https://doi.org/10.1111/j.1752-1688.1989.tb05402.x

Redfield, A. C. (1972), Development of a New England Salt Marsh. *Ecological Monographs*, 42: 201-237. doi:10.2307/1942263

Ridderinkhof, H., van der Ham, R., and van der Lee, W. (2000). Temporal variations in concentration and transport of suspended sediments in a channel–flat system in the Ems-Dollard estuary. *Continental Shelf Research*, *20*(12), 1479–1493. https://doi.org/10.1016/S0278-4343(00)00033-9

Roman, C. T. (1984). Estimating water volume discharge through salt-marsh tidal channels: An aspect of material exchange. *Estuaries*, *7*(3), 259–264. https://doi.org/10.2307/1352146

Scarborough, R. W. (2009). Application of the Sea Level Rise Affecting Marsh Model (SLAMM) Using High Resolution Data at Prime Hook National Wildlife Refuge. DNREC, DSWC, Delaware Coastal Programs. Retrieved from http://www.dnrec.delaware.gov/coastal/Documents/PHNWR%20SLAMM.pdf

Scavia, D., Field, J. C., Boesch, D. F., Buddemeier, R. W., Burkett, V., Cayan, D. R., Fogarty, M., Harwell, M. A., Howarth, R. W., Mason, C., Reed, D. J., Royer, T.C., Sallenger, A. H., Titus, J. G. (2002). Climate change impacts on U.S. Coastal and Marine Ecosystems. Estuaries, 25(2), 149–164. https://doi.org/10.1007/BF02691304

SondeTek. (2018) *SondeTek-SL User's Manual*. San Diego, CA. 2018. Retrieved from http://info.xylem.com/SonTek-SLManual.html?_ga=2.138117680.1049736291.1564681920-159146082.1564681920

Stevenson, J. C., Ward, L. G., and Kearney, M. S. (1986). Vertical Accretion in Marshes with Varying Rates of Sea Level Rise. Wolfe, Douglas A. In *Estuarine Variability* (pp. 241–259). Academic Press. https://doi.org/10.1016/B978-0-12-761890-6.50020-4

Stevenson, J. C., Ward, L. G., and Kearney, M. S. (1988). Sediment transport and trapping in marsh systems: Implications of tidal flux studies. *Marine Geology*, *80*(1), 37–59. https://doi.org/10.1016/0025-3227(88)90071-0

Sturdevant, A., Craft, C. B., and Sacco, J. N. (2002). Ecological functions of an impounded marsh and three natural estuarine marshes along Woodbridge River, NY/NJ Harbor. *Urban Ecosystems*, *6*(3), 163–181. https://doi.org/10.1023/A:1026356211862

Sussex County Planning & Zoning Commission. (2019). *Sussex County Comprehensive Plan*. https://sussexcountyde.gov/sites/default/files/PDFs/2018CompPlan-Final.pdf

Tiner, R.W., M.A. Biddle, A.D. Jacobs, A.B. Rogerson and K.G. McGuckin. (2011). *Delaware Wetlands: Status and Changes from 1992 to 2007.* Cooperative National Wetlands Inventory Publication. U.S. Fish and Wildlife Service, Northeast Region, Hadley, MA and the Delaware Department of Natural Resources and Environmental Control, Dover, DE. 35 pp. Retrieved from http://www.dnrec.delaware.gov/Admin/DelawareWetlands/Documents/Delaware%20Wetlands%20Status%20and%20Changes%20from%201992%20to%202007%20FINAL2012.pdf

U.S. Department of Agriculture (2012). *Delaware State and County Data*. Retrieved from https://www.nass.usda.gov/Publications/AgCensus/2012/Full_Report/Volume_1,_Chapter_2_County_Level/Delaware/dev1.pdf

U.S. EPA. (2019) Application of the Sea-Level Affecting Marshes Model (SLAMM) to the Lower Delaware Bay, with a Focus on Salt Marsh Habitat. *U.S. Environmental Protection Agency*, Washington, DC, EPA/600/R-18/385. Retrieved from https://cfpub.epa.gov/ncea/global/recordisplay.cfm?deid=344746

U.S. Fish & Wildlife Service (2012). *Hurricane Sandy impacts Prime Hook National Wildlife Refuge (DE)*. Retrieved from https://www.flickr.com/photos/usfwsnortheast/8148591065/

U.S. Fish & Wildlife Service (2013). *Prime Hook National Wildlife Refuge Comprehensive Conservation Plan*. Retrieved from https://www.fws.gov/refuge/Prime_Hook/what_we_do/finalccp.html

"USFWS Prime Hook Water Quality Metadata" (2019). Delaware Coastal Programs/National Estuarine Research Reserve Program.

Weston, N. B. (2014). Declining Sediments and Rising Seas: an Unfortunate Convergence for Tidal Wetlands. *Estuaries and Coasts*, *37*(1), 1–23. https://doi.org/10.1007/s12237-013-9654-8

Whiting, G. J. and Chanton, J. P. (2001), Greenhouse carbon balance of wetlands: methane emission versus carbon sequestration. *Tellus B*, 53: 521-528. Retrieved from https://doi.org/10.1034/j.1600-0889.2001.530501.x

Wilson, B., Guiteras, S., Rizzo, A. and Coppola, A. (2017). Large Scale Coastal Tidal Marsh and Barrier Beach Restoration at Prime Hook NWR - Recovering from Hurricane Sandy and Building Resilience in Former Freshwater Impoundments. Retrieved from https://fws.rev.vbrick.com/#/videos/560220a6-6594-4967-a8d9-1d62dd78caa4

Wolaver, T. G., Dame, R. F., Spurrier, J. D., and Anne B. Miller. (1988). Sediment Exchange between a Euhaline Salt Marsh in South Carolina and the Adjacent Tidal Creek. *Journal of Coastal Research*, *4*(1), 17–26. Retrieved from http://journals.fcla.edu/jcr/article/view/77677/75134

Zedler, J. B. & Kercher, S. (2005). Wetland Resources: Status, Trends, Ecosystem Services, and Restorability. Annual Review. *Environmental Resources*. 15. 39-74. Retrieved from https://doi.org/10.1146/annurev.energy.30.050504.144248

Appendix A

SUPPLEMENTARY DATA

Meteorological Data

Daily Averaged Wind Speed (m/s)				Precipitation (cm)			
Min	Max	Mean	St Dev	Min	Max	Mean	St Dev
0.313	6.527	2.134	1.116	0	6.958	0.370	0.924

Autocorrelations of Precipitation and Site Discharge

SCB		FBR	
Lag	Correlation Coefficient	Lag	Correlation Coefficient
-10	0.007	-10	-0.007
-9	0.069	-9	0.011
-8	-0.003	-8	0.058
-7	0.053	-7	0.049
-6	0.064	-6	0.098
-5	0.139*	-5	0.026
-4	0.215*	-4	0.094
-3	0.330*	-3	0.221*
-2	0.169*	-2	0.200*
-1	0.248*	-1	0.078
0	-0.055	0	0.070
1	-0.078	1	-0.024
2	-0.156	2	0.006
3	-0.075	3	0.058
4	-0.022	4	0.019
5	0.069	5	-0.082
6	0.060	6	-0.122
7	-0.068	7	-0.060
8	-0.003	8	0.005
9	-0.015	9	-0.009
10	-0.064	10	0.019
PFD		BKR	
Lag	Correlation Coefficient	Lag	Correlation Coefficient
-10	-0.007	-10	-0.028
-9	0.011	-9	0.021
-8	0.043	-8	0.054
-7	0.049	-7	0.029
-6	-0.010	-6	0.034
-5	0.085	-5	0.110*
-4	0.066	-4	0.219*

-3	0.157*	-3	0.263*
-2	0.253*	-2	0.261*
-1	0.1241*	-1	0.095
0	0.092	0	0.00
1	-0.050	1	-0.120
2	-0.077	2	-0.131
3	0.068	3	-0.135
4	0.056	4	-0.116
5	0.007	5	-0.020
6	-0.021	6	-0.019
7	-0.114	7	-0.071
8	-0.063	8	-0.158
9	-0.022	9	-0.051
10	0.043	10	0.009

* Indicates significance